HNPS Advances in Nuclear Physics
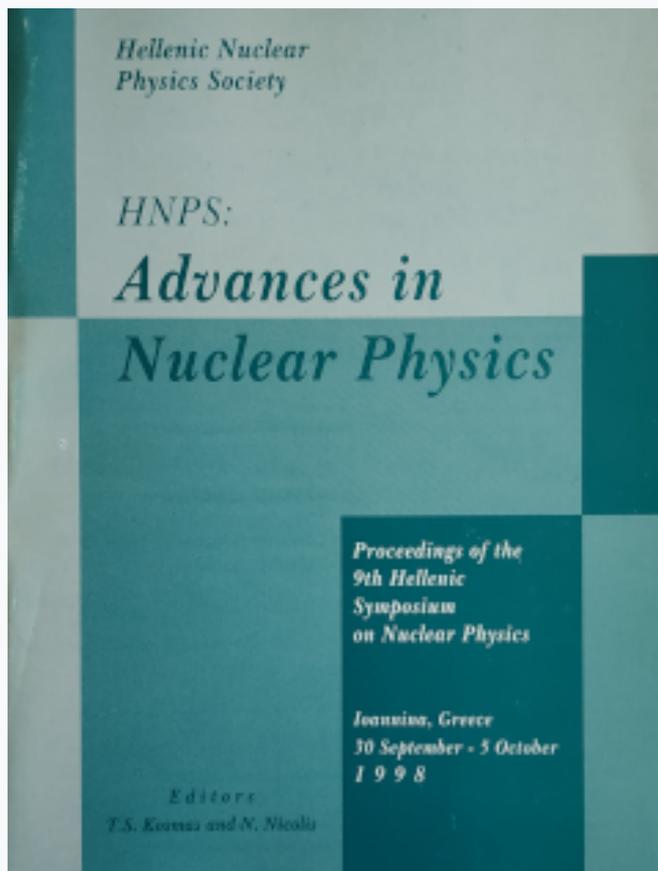
Chiral symmetries in nuclear physics

D. Zschiesche, P. Papazoglou, S. Schramm, W. Ch. Beckmann, J. Schaffner-Bielich, H. Stöcker, W. Greiner

Chiral symmetries in nuclear physics

D. Zschiesche [a] P. Papazoglou [a] S. Schramm [b]
W. Ch. Beckmann [a] J. Schaffner-Bielich [c] H. Stöcker [a]
W. Greiner [a]

[a] *Institut für Theoretische Physik, Postfach 11 19 32 D-60054 Frankfurt am Main, Germany*

[b] *GSI Darmstadt, Postfach 11 05 52, D-64220 Darmstadt, Germany*

[c] *Riken BNL Research Center, Brookhaven National Lab, Upton, New York 11973*

Abstract

In this report the theoretical concepts of a chirally symmetric meson field theory are reviewed and an overview of the most relevant applications in nuclear physics is given. This includes a unified description of the vacuum properties of hadrons, finite nuclei and hot, dense and strange nuclear matter in an extended chiral $SU(3)_L \times SU(3)_R$ $\sigma - \omega$ model.

1 Introduction - General Ideas

Quantum Chromodynamics (QCD) is the accepted theory of strong interactions, but for low energies it is not perturbatively solvable. One idea to overcome this problem is lattice gauge theory, where QCD is solved numerically on a finite space-time lattice. So far, lattice gauge theory is not able to describe finite nuclei or dense nuclear matter (finite chemical potential) [1]. A different approach has been followed in nuclear physics for several years that is well known from other disciplines, the idea of constructing effective theories. In this concept only the relevant degrees of freedom for the problem are considered to construct a simplified model which is solvable, but contains the interesting and essential characteristics of the full theory. For the case of strong interactions this means that one considers the hadrons as relevant degrees of freedom instead of quarks, and the bosonic fields are mesons instead of gluons. There exist several models which successfully describe nuclear matter and finite nuclei in such a way [2–4]. Especially the Walecka model (QHD) and its extensions (QHD II, nonlinear Walecka model) have been very successful and widely used for the description of hadronic matter and finite nuclei.

These models are relativistic quantum field theories of baryons and mesons, but do not consider some of the essential features of QCD, like approximate $SU(3) \times SU(3)$ chiral symmetry or broken scale invariance. This lead us to construct an extended chiral $SU(3)$ $\sigma - \omega$ model of hadrons and mesons, which on one hand incorporates the successful idea that the strong interaction is mediated by scalar- and vector mesons and which on the other hand contains the relevant symmetries of QCD. In this paper the basic concepts, the Lagrangian and the main applications of this model will be reported. In Sec. 2 we discuss the motivation for using chiral symmetry in effective models for strongly interacting matter. Section 3 shows the representations and transformations of the chiral $SU(3) \times SU(3)$ group. The nonlinear realization of chiral symmetry and the resulting transformation properties of the relevant degrees of freedom are considered in Sec. 4. The chiral $SU(3)$ Lagrangian is constructed and discussed in Sec. 5. The equations of motion are solved in the mean field approximation (Sec. 6). In Sec. 7 we demonstrate that vacuum properties of hadrons and nuclear matter ground state properties can be described satisfactorily in the chiral $SU(3)$ model. Finally, two main applications are presented. Section 8 shows the results for nuclei, hypernuclei and superheavies and in Sec. 9 the extension to hot and dense hadronic matter is discussed. The conclusions will be drawn in Sec. 10.

2   Why Chiral Symmetry ?

Recently, the general principles of chiral symmetry and broken scale invariance in QCD have received renewed attention at finite baryon densities. There are several reasons for this. First of all in an effective theory of strong interactions, the main features of QCD should be implemented. One important part of these features are symmetries. Lorentz invariance, parity invariance and more are already incorporated in QHD. But chiral symmetry and the broken scale invariance have not been accounted for, even though $SU(2) \times SU(2)$ chiral symmetry is a very good symmetry of QCD and $SU(3) \times SU(3)$ chiral symmetry, even though it is stronger broken due to the strange quark mass, can still be considered as an explicitly broken symmetry. In this spirit, models with $SU(2)_L \times SU(2)_R$ symmetry and scale invariance were applied to nuclear matter at zero and finite temperature and to finite nuclei [5–9]. As a new feature, a glueball field χ, the dilaton, was included, which accounted for the broken scale invariance of QCD at tree level through a logarithmic potential [10]. The success of these models established the applicability of this approach to the relativistic description of the nuclear many-body problem. Chiral $SU(3)$ models have been quite successful in describing hadron interactions, e.g. meson-meson interactions can be described very well by using the linear $SU(3)$ σ model [11] and Kaon-nucleon scattering can be well described

using a chiral effective $SU(3)$ Lagrangian [12,13]. But these models lack the feature of including the nucleon-nucleon interaction on the same chiral $SU(3)$ basis and therefore do not allow a consistent extrapolation to finite density. Therefore we have extended the chiral effective model to $SU(3)_L \times SU(3)_R$ [14,15]. This approach shall provide a basis to shed light on the properties of strange hadrons, as the in-medium properties of the hadrons and the properties of strange hadronic matter, by pinning down the nuclear force in a chirally invariant way. It has been found that simultaneously hadronic masses of the various $SU(3)$ multiplets, the nuclear matter equation of state, finite nuclei, hypernuclei and excited nuclear matter can be described reasonably well within a model respecting chiral symmetry.

3 $SU(3) \times SU(3)$

The σ-model has been used extensively in exploring the implications of chiral symmetry in low-energy hadron dynamics. Most of these investigations have employed the $SU(2)$ model with mesons and nucleons and the $SU(3)$ σ-model with mesons only. We require the effective model for hadronic matter to be approximately $SU(3) \times SU(3)$ chirally invariant and include baryons, spin-0 and spin-1 mesons, where the latter are necessary for non-zero baryon densities. Therefore, in this section we will discuss the transformation properties of spin-0 and spin-1 mesons as well as of the baryons. First, we determine the group representations to the various hadronic multiplets.

3.1   Representations

For determining the representations to which the hadrons are assigned, we will look at their quark content. The representations of the hadrons result from the direct product of the quark representations. However, in the Lagrangian, there will be no explicit reference to quarks. For our purpose, they are only used as a pedagogical and mnemonic tool. In the chiral limit, the quarks are massless. Therefore, it is sufficient to consider the 2-component spinors

$$q_L = \frac{1}{2}(1 - \gamma_5)q \quad \sim \quad (3,0)\,, \nu_1 \tag{1}$$

$$q_R = \frac{1}{2}(1 + \gamma_5)q \quad \sim \quad (0,3)\,. \tag{2}$$

Since the quarks are massless, the chirality of the spinors is linked to their spin. On the right-hand side, the quark representations are symbolized by the

number of flavors, which is placed left (right) from the comma between the brackets for the left (right) subspace.

3.1.1 Mesons

The mesons visualized as a bound system of a quark and antiquark correspond to the bilinear form $\bar{q}\mathcal{O}q$ where the 12×12 matrix $\mathcal{O}$ is the direct product of the 4×4 Dirac matrices and the 3×3 unitary spin matrices ($\mathcal{O} = \Gamma \otimes \lambda$). For the discussion of the representations we will first suppress the explicit reference to the Gell-Mann matrix λ.

First, consider the spin-0 mesons. Assuming that they are s-wave bound states, then the only spinless objects we can form are

$$\bar{q}_R q_L , \quad \bar{q}_L q_R . \tag{3}$$

The combinations $\bar{q}_L q_L$ and $\bar{q}_R q_R$ vanish, since the left and right subspaces are orthogonal to each other. The resulting representation is $(3, 3^*)$ and $(3^*, 3)$, respectively (The antiparticles belong to the conjugate representation). We are thus led to consider nonets of pseudoscalar and scalar particles.

For the vector mesons, we have to construct vectorial quantities out of q_L and q_R. Again, if we assume that s-wave bound states are involved, the only vectors which can be formed are

$$\bar{q}_L \gamma_\mu q_L , \quad \bar{q}_R \gamma_\mu q_R . \tag{4}$$

This suggests assigning the vector and axial vector mesons to the representation $(3 \times 3^*, 0) \oplus (0, 3 \times 3^*) = (8, 1) \oplus (1, 8)$, coinciding with the tensor properties of the currents conserved in the $SU(3) \times SU(3)$ limit [16,17].

3.1.2 Baryons

The representation of spin-$\frac{3}{2}$-baryons can be obtained from the symmetric coupling of three left- or right-handed quarks, $(3 \times 3 \times 3, 0) = (10, 0)$ or $(0, 3 \times 3 \times 3) = (0, 10)$. For spin-$\frac{1}{2}$ particles the construction of baryon multiplets from the basic fields q_L and q_R is not unique. The reason is that a left- or right-handed quark can be added to the spin-0 diquark of one subspace. Consequently, the baryons can be assigned to the representation $(3, 3^*)$ and $(3^*, 3)$ or $(8, 1)$ and $(1, 8)$, respectively. For an explicit construction in terms of quark fields see [18,19].

Once the chiral transformations properties of the elementary spinors are known it is straightforward to derive the corresponding transformations properties of the composite fields.

An arbitrary element of $SU(3) \times SU(3)$ can be written as

$$U(\alpha, \beta) = e^{(-[i\alpha_a Q^a + i\beta_a Q^{5a}])} = e^{(-i[(\alpha+\beta) \cdot Q_L + (\alpha-\beta) \cdot Q_R])} , \tag{5}$$

where α and β are eight-component vectors, and Q, Q^5 are the vector and axial generators, respectively. The spinor q_L transforming under $SU(3)_L$ generated by Q_L and q_R of $SU(3)_R$ generated by Q_R transform infinitesimally as

$$q_i \longrightarrow q_i + i\left[(\alpha + \beta) \cdot \lambda/2\right]_i^j q_j , \tag{6}$$

$$q_{\bar{i}} \longrightarrow q_{\bar{i}} + i\left[(\alpha - \beta) \cdot \lambda/2\right]_{\bar{i}}^{\bar{j}} q_{\bar{j}} . \tag{7}$$

Here, the (un-)barred indices belong to the (right) left subspace. Since the Gell-Mann matrices are hermitean, the complex conjugate spinor transforms as

$$q^i \longrightarrow q^i - iq^j \left[(\alpha + \beta) \cdot \lambda/2\right]_j^i . \tag{8}$$

Knowing the representation of the mesonic and baryonic fields, it is straightforward to derive their transformation properties. They are summarized in Table 1, where we conveniently express the fields in a basis of 3×3 Gell-Mann matrices. For example, the spin-0 mesons may be written in the compact form

$$\sum_{a=0}^{8} (\overline{q}_L \lambda^a q_R + \overline{q}_L \lambda^a \gamma_5 q_R) \equiv \sum_{a=0}^{8} (\xi_a \lambda_a + i\pi_a \lambda_a) = \Sigma + i\Pi = M$$

$$\sum_{a=0}^{8} (\overline{q}_R \lambda^a q_L + \overline{q}_R \lambda^a \gamma_5 q_L) \equiv \sum_{a=0}^{8} (\xi_a \lambda_a - i\pi_a \lambda_a) = \Sigma - i\Pi = M^\dagger .$$

The first and second row are connected by the parity transformation, which transforms left-handed quarks to right handed ones. In the matrix formulation this is achieved by taking the adjoint of the expression. Therefore, since scalar and pseudoscalar particles have opposite parity, an imaginary unit i is attached to the pseudoscalar matrix Π.

Table 1
Chiral transformations of spin-0 mesons ($M = \Sigma + i\Pi$), spin-1 mesons ($V_\mu = l_\mu + r_\mu$ and $A_\mu = l_\mu - r_\mu$) and baryons

Hadrons	J^P	Transformations	
Spin-0 mesons	$0^+, 0^-$	$LMR^\dagger$	$RM^\dagger L^\dagger$
Spin-1 mesons	$1^-, 1^+$	$Ll_\mu L^\dagger$	$Rr_\mu R^\dagger$
baryons (spin-$\frac{1}{2}$-nonet)	$\frac{1}{2}^+$	$L\Psi_L R^\dagger$	$R\Psi_R L^\dagger$
baryons (spin-$\frac{1}{2}$-octet)	$\frac{1}{2}^+$	$L\Psi_L L^\dagger$	$R\Psi_R R^\dagger$
baryons (spin-$\frac{3}{2}$-decuplet)	$\frac{3}{2}^+$	$LLL\Delta_L$	$RRR\Delta_R$

4 The nonlinear realization of chiral symmetry

In some neighborhood of the identity transformation, every group element $g'(x)$ of a compact, semi-simple group G with a subgroup H can be decomposed uniquely into a product of the form [20]

$$g'(x) = \exp\left[i\sum \xi_a(x)x_a\right] \exp\left[i\sum \theta_b(x)t_b\right] \equiv u\left(\xi_a(x)\right) h\left(\theta_b(x)\right) , \qquad (9)$$

where $h(\theta_b)$ is an element of H, ξ_a and θ_b are parameters of the symmetry transformation which are generally space-time dependent, x_a and t_b represent the generators of the group G.

For the case of $SU(3)_L \times SU(3)_R$ symmetry, the generators are the vectorial ($t_i = Q_i$) and axial ($x_i = Q_i^5$) charges, respectively, and the subgroup is $H = SU(3)_V$.

For our model, we assume invariance under *global* $SU(3)_L \times SU(3)_R$ transformations,

$$g = \exp\left[i\sum \alpha_L^a \lambda_{La}\right] \exp\left[i\sum \alpha_R^b \lambda_{Rb}\right] \equiv L\left(\alpha_L\right) R\left(\alpha_R\right) . \qquad (10)$$

Here, the representation of Gell-Mann matrices $\lambda_L = \lambda(1 - \gamma_5)/2$ and $\lambda_R = \lambda(1 + \gamma_5)/2$ with space-time independent parameters α_L and α_R is used.

The product $g\, u(\xi_a(x))$ is still an element of G and can be written as

$$g \exp\left[i\sum \xi_a x_a\right] = \exp\left[i\sum \xi_a'(g, \xi_a)x_a\right] \exp\left[i\sum \theta_b'(g, \xi_a)t_b\right] , \qquad (11)$$

where, in general, both ξ_a' and θ_b' depend on g and ξ_a. Let

$$\tilde{q} \to D(h)\tilde{q} \qquad (12)$$

be a linear representation of the subgroup H of G. Then the transformation

$$g : \xi \rightarrow \xi', \tilde{q} \rightarrow D \left(\exp \left[i \sum \theta'_b t_b \right] \right) \tilde{q} \tag{13}$$

constitutes a nonlinear realization of G.

The local parameters of the axial charges are identified with the fields of the pseudoscalar mesons [21]. In the representation of Gell-Mann matrices one has (see also Appendix A)

$$u(\pi_a(x)) = \exp \left[\frac{i}{2\sigma_0} \pi^a(x) \lambda_a \gamma_5 \right] . \tag{14}$$

This assignment has the advantage that the pseudoscalar mesons are the parameters of the symmetry transformation. They will therefore only appear if the symmetry is explicitly broken or in terms with derivatives of the fields.

The composition of hadrons in terms of its constituents, the quarks, has to be determined in order to build models with hadronic degrees of freedom. This strategy has been followed e.g. in [14] and is adopted also here. The transformation properties of the hadrons in the nonlinear representation can be derived if the 'old' quarks q are related to the 'new' quarks $\tilde{q}$ of the nonlinear representation.

The quarks of the nonlinear representation transform with the vectorial subgroup $SU(3)_V$ in accord with (9). Splitting the quarks in left- and right-handed parts, they can be written as

$$q_L = u\tilde{q}_L \qquad q_R = u^\dagger \tilde{q}_R . \tag{15}$$

These equations are connected by parity. The ambiguity in the choice of h is avoided by setting $h = 1$. The transformation properties of the pions and the new quarks are found by considering how the old quarks transform:

$$q' = Lq_L + Rq_R = Lu\tilde{q}_L + Ru^\dagger\tilde{q}_R . \tag{16}$$

According to (11), (set $g = L$),

$$Lu = u'h \quad ; \quad Ru^\dagger = u^{\dagger\prime}h , \tag{17}$$

where the right equation is the parity transformed one of the left equation. Here and in the following, the abbreviations $u \equiv u(\pi_a(x))$ and $u' \equiv u(\pi'_a(x))$

176

are used. By inserting these relations into (16), one sees that $\tilde{q}$ transforms with $SU(3)_V$ as

$$\tilde{q}'_L = h\tilde{q}_L \quad ; \quad \tilde{q}'_R = h\tilde{q}_R . \tag{18}$$

According to (11), in general the vector transformation is a local, nonlinear function depending on pseudoscalar mesons, $h = h(g, \pi_a(x))$. Following equation (17), the pseudoscalar mesons transform nonlinearly as

$$u' = Luh^\dagger = huR^\dagger , \tag{19}$$
$$u^\dagger = hu^\dagger L^\dagger = Ru^\dagger h^\dagger . \tag{20}$$

The second set of equalities are again due to parity. In contrast to the linear realization of chiral symmetry, there is no distinction between the left and right space. Therefore, only the representations **8** and **1** of the lowest-lying hadrons are possible. The various octets transform accordingly, e.g. for the scalar (X), vector ($V_\mu = l_\mu + r_\mu$), axial vector ($\mathcal{A}_\mu = l_\mu - r_\mu$) and baryon ($B, D$) matrices one has,

$$X' = hXh^\dagger, \ V'_\mu = hV_\mu h^\dagger, \ \mathcal{A}'_\mu = h\mathcal{A}_\mu h^\dagger, \ B' = hBh^\dagger, \ D' = hhhD . \tag{21}$$

The present, nonlinearly transforming, hadronic fields can be obtained from the linearly transforming ones described in [14] by multiplying them with $u(\pi(x))$ and its conjugate: (see also [22])

$$X = \frac{1}{2}(u^\dagger M u^\dagger + u M^\dagger u) , \quad Y = \frac{1}{2}(u^\dagger M u^\dagger - u M^\dagger u) , \tag{22}$$
$$l_\mu = u^\dagger \tilde{l}_\mu u , \quad r_\mu = u\tilde{r}_\mu u^\dagger , \tag{23}$$
$$B_L = u^\dagger \Psi_L u , \quad B_R = u\Psi_R u^\dagger , \tag{24}$$
$$D_L = uuu\Delta_R , \quad D_R = u^\dagger u^\dagger u^\dagger \Delta_L . \tag{25}$$

Here, $M = \Sigma + i\Pi$ and its conjugate contains the nonets of the linearly transforming scalar (Σ) and pseudoscalar (Π) mesons, whereas $\tilde{l}_\mu$, $\tilde{r}_\mu$, Ψ_L, Ψ_R, Δ_L and Δ_R are the left and right-handed parts of the spin-1 mesons, spin-$\frac{1}{2}$ baryons and spin-$\frac{3}{2}$ baryons in the linear representation, respectively.

5 Lagrangian

In this section, the various terms of the Lagrangian

$$\mathcal{L} = \mathcal{L}_{\text{kin}} + \sum_{W=X,Y,V,\mathcal{A},u} \mathcal{L}_{BW} + \mathcal{L}_{VP} + \mathcal{L}_{\text{vec}} + \mathcal{L}_0 + \mathcal{L}_{\text{SB}} \tag{26}$$

are discussed in detail. $\mathcal{L}_{\text{kin}}$ is the kinetic energy term of baryons (spin-$\frac{1}{2}$ and spin-$\frac{3}{2}$) and mesons (spin-0 and spin-1), $\mathcal{L}_{BW}$ includes the interaction terms of the different baryons with the various spin-0 and spin-1 mesons. $\mathcal{L}_{\text{vec}}$ generates the masses of the spin-1 mesons through interactions with spin-0 mesons, and $\mathcal{L}_0$ gives the meson-meson interaction terms which induce the spontaneous breaking of chiral symmetry. It also includes the scale breaking logarithmic potential. Finally, $\mathcal{L}_{\text{SB}}$ introduces an explicit symmetry breaking of the $U(1)_A$, the $SU(3)_V$, and the chiral symmetry.

Baryon-meson interaction

The various interaction terms of baryons with mesons are discussed in this section. The $SU(3)$ structure of the the spin-$\frac{1}{2}$ baryon-meson interaction terms are the same for all mesons, except for the difference in Lorentz space. For a general meson field W they read

$$\mathcal{L}_{OW} = -\sqrt{2}g_{O8}^W \left(\alpha_{OW}[\overline{B}OBW]_F + (1-\alpha_{OW})[\overline{B}OBW]_D \right) \nu_1 \tag{27}$$

$$-g_{O1}^W \frac{1}{\sqrt{3}} \text{Tr}(\overline{B}OB)\text{Tr}W , \tag{28}$$

with $[\overline{B}OBW]_F := \text{Tr}(\overline{B}OWB - \overline{B}OBW)$ and $[\overline{B}OBW]_D := \text{Tr}(\overline{B}OWB + \overline{B}OBW) - \frac{2}{3}\text{Tr}(\overline{B}OB)\text{Tr}W$. The different terms to be considered are those for the interaction of spin-$\frac{1}{2}$ baryons, with scalar mesons ($W = X, O = 1$), with vector mesons ($W = V_\mu, O = \gamma_\mu$ for the vector and $W = V_{\mu\nu}, O = \sigma^{\mu\nu}$ for the tensor interaction), with axial vector mesons ($W = \mathcal{A}_\mu, O = \gamma_\mu\gamma_5$) and with pseudoscalar mesons ($W = u_\mu, O = \gamma_\mu\gamma_5$), respectively. For the spin-$\frac{3}{2}$ baryons one can construct a coupling term similar to (28)

$$\mathcal{L}_{DW} = -\sqrt{2}g_{D8}^W \alpha_{DW}[\overline{D^\mu}OD_\mu W] - g_{D1}^W[\overline{D^\mu}OD_\mu]TrW , \tag{29}$$

where $[\overline{D^\mu}OD_\mu W]$ and $[\overline{D^\mu}OD_\mu W]$ are obtained from coupling $[\overline{10}] \times [10] \times [8]$ and $[\overline{10}] \times [10] \times [1]$ to an $SU(3)$ singlet, respectively.

In the following we will discuss the couplings of the baryons to the scalar and vector mesons. For the pseudoscalar mesons only a pseudovector coupling is possible, since they only appear in the exponentials. Pseudovector and axial mesons have a vanishing expectation value at the mean field level, so that their coupling terms will not be discussed in detail here.

5.1 Scalar mesons

The baryons and the scalar mesons transform equally in the left and right subspace. Therefore, in contrast to the linear realization of chiral symmetry, a f-type coupling is allowed for the baryon-octet-meson interaction. In addition, it is possible to construct mass terms for baryons and to couple them to chiral singlets.

After insertion of the vacuum matrix $\langle X \rangle$, (A.6), one obtains the baryon masses as generated by the vacuum expectation value (VEV) of the two meson fields:

$$m_N = m_0 - \frac{1}{3}g_{O8}^S(4\alpha_{OS} - 1)(\sqrt{2}\zeta - \sigma) \,, \nu_1$$

$$m_\Lambda = m_0 - \frac{2}{3}g_{O8}^S(\alpha_{OS} - 1)(\sqrt{2}\zeta - \sigma) \,, \nu_1$$

$$m_\Sigma = m_0 + \frac{2}{3}g_{O8}^S(\alpha_{OS} - 1)(\sqrt{2}\zeta - \sigma) \,, \nu_1$$

$$m_\Xi = m_0 + \frac{1}{3}g_{O8}^S(2\alpha_{OS} + 1)(\sqrt{2}\zeta - \sigma) \,,$$

with $m_0 = g_{O1}^S(\sqrt{2}\sigma + \zeta)/\sqrt{3}$. The parameters g_{O1}^S, g_{O8}^S and α_{OS} can be used to fit the baryon masses to their experimental values. Besides the current quark mass terms discussed in Sec. 5.6, no additional explicit symmetry breaking term is needed. Note that the nucleon mass depends on the *strange conden-sate* ζ! For $\zeta = \sigma/\sqrt{2}$ (i.e. $f_\pi = f_K$), the masses are degenerate, and the vacuum is $SU(3)_V$-invariant. For the spin-$\frac{3}{2}$ baryons the procedure is similar. If the vacuum matrix for the scalar condensates is inserted one obtains the dynamically generated vacuum masses of the baryon decuplet

$$m_\Delta = g_D^S\left[(3 - \alpha_{DS})\sigma + \alpha_{DS}\sqrt{2}\zeta\right] \,, \nu_1$$

$$m_{\Sigma^*} = g_D^S\left[2\sigma + \sqrt{2}\zeta\right] \,, \nu_1$$

$$m_{\Xi^*} = g_D^S\left[(1 + \alpha_{DS})\sigma + (2 - \alpha_{DS})\sqrt{2}\zeta\right] \,, \nu_1$$

$$m_\Omega = g_D^S\left[\alpha_{DS}\sigma + (3 - \alpha_{DS})\sqrt{2}\zeta\right] \,.$$

The parameters g_D^S and α_{DS} are fixed to reproduce the masses of the baryon decuplet. As in the case of the nucleon, the coupling of the Δ to the strange condensate is nonzero.

It is desirable to have an alternative way of baryon mass generation, where the nucleon and the Δ mass depend only on σ. For the nucleon this can be accomplished for example by taking the limit $\alpha_{OS} = 1$ and $g_{O1}^S = \sqrt{6}g_{O8}^S$. Then, the coupling constants between the baryon octet and the two scalar condensates are related to the additive quark model. This leaves only one coupling constant to adjust for the correct nucleon mass. For a fine-tuning of the remaining masses, it is necessary to introduce an explicit symmetry breaking term, that breaks the $SU(3)$-symmetry along the hypercharge direction. A possible term already discussed in [14,23], which respects the Gell-Mann-Okubo mass relation, is

$$\mathcal{L}_{\Delta m} = -m_1 \text{Tr}(\overline{B}B - \overline{B}BS) - m_2 \text{Tr}(\overline{B}SB) , \tag{30}$$

where $S_b^a = -\frac{1}{3}[\sqrt{3}(\lambda_8)_b^a - \delta_b^a]$. As in the first case, the three coupling constants $g_{N\sigma} \equiv 3g_{O8}^S$, m_1 and m_2 are sufficient to reproduce the experimentally known baryon masses. Explicitly, the baryon masses have the values

$$m_N = -g_{N\sigma}\sigma \,, \nu_1$$
$$m_\Xi = -\frac{1}{3}g_{N\sigma}\sigma - \frac{2}{3}g_{N\sigma}\sqrt{2}\zeta + m_1 + m_2 \,, \nu_1$$
$$m_\Lambda = -\frac{2}{3}g_{N\sigma}\sigma - \frac{1}{3}g_{N\sigma}\sqrt{2}\zeta + \frac{m_1 + 2m_2}{3} \,, \nu_1$$
$$m_\Sigma = -\frac{2}{3}g_{N\sigma}\sigma - \frac{1}{3}g_{N\sigma}\sqrt{2}\zeta + m_1 .$$

For the baryon decuplet one can choose $\alpha_{DS} = 0$ to obtain coupling constants related to the additive quark model. We introduce an explicit symmetry breaking proportional to the number of strange quarks for a given baryon species. Here we need only one additional parameter m_{Ds} to obtain the masses of the baryon decuplet:

$$m_\Delta = g_{\Delta\sigma}[3\sigma] \,, \nu_1$$
$$m_{\Sigma^*} = g_{\Delta\sigma}[2\sigma + \sqrt{2}\zeta] + m_{Ds} \,, \nu_1$$
$$m_{\Xi^*} = g_{\Delta\sigma}[1\sigma + 2\sqrt{2}\zeta] + 2m_{Ds} \,, \nu_1$$
$$m_\Omega = g_{\Delta\sigma}[0\sigma + 3\sqrt{2}\zeta] + 3m_{Ds} .$$

For both versions of the baryon-meson interaction the parameters are fixed to yield the baryon masses of the octet and the decuplet (Table 2 and 3).

Table 2
Hadron masses (in MeV) for the different fits C_1, C_2, C_3

				Spin-0 particle masses				
	m_π	m_K	m_η	$m_{\eta'}$	m_{a_0}	m_κ	m_σ	m_{f_0}
	(139)	(495)	(547)	(958)	(980)	(900)		(980)
C_1	139.0	498.0	574.5	969.2	953.5	995.7	473.32	1039.1
C_2	139.0	498.0	574.5	969.2	953.5	995.7	475.55	1039.1
C_3	139.0	498.0	574.5	969.2	953.5	995.7	478.56	824.17

		Spin-1 particle masses			Spin-$\frac{1}{2}$ particle masses			
	m_ω	m_{K^*}	m_ρ	m_ϕ	m_N	m_Λ	m_Σ	m_Ξ
	(783)	(892)	(770)	(1020)	(939)	(1115)	(1193)	(1315)
C_1	783.0	863.7	770.0	1019.0	939.0	1115.0	1196.0	1331.5
C_2	783.0	863.7	770.0	1019.0	939.0	1115.3	1196.0	1331.5
C_3	783.0	863.7	770.0	1019.0	939.0	1115.0	1196.0	1331.5

Table 3
Vacuum masses of baryon resonances and baryonic potential depths in nuclear matter

	m_Δ	m_{Σ^*}	m_{Ξ^*}	m_Ω	$\frac{m_N^*}{m_N}$	K [MeV]	U_N	U_Λ
C_1	1232.0	1380.0	1527.9	1675.8	0.61	276.3	-71.0	-28.2
C_2	1232.0	1380.2	1528.4	1676.6	0.64	266.1	-68.8	-30.5
C_3	1232.0	1380.0	1527.9	1675.8	0.61	285.3	-71.1	-28.61

5.2 Vector mesons

For the spin-$\frac{1}{2}$ baryons two independent interaction terms with spin-1 mesons can be constructed in analogy to the interaction of the baryon octet with the scalar mesons. They correspond to the antisymmetric (f-type) and symmetric (d-type) couplings, respectively. From the universality principle [24] and the vector meson dominance model one may conclude that the d-type coupling should be small. For most of the fits $\alpha_V = 1$, i.e. f-type coupling, is used. However, a small admixture of d-type coupling allows for some fine-tuning of the single-particle energy levels of nucleons in nuclei [15]. As for the case of scalar mesons, for $g_{O1}^V = \sqrt{6}g_{O8}^V$, the strange vector field $\phi_\mu \sim \bar{s}\gamma_\mu s$ does not couple to the nucleon. The remaining couplings to the strange baryons are

181

then determined by symmetry relations:

$$g_{N\omega} = (4\alpha_V - 1)g_{O8}^V \ , \nu_1$$

$$g_{\Lambda\omega} = \frac{2}{3}(5\alpha_V - 2)g_{O8}^V \ , \qquad g_{\Lambda\phi} = -\frac{\sqrt{2}}{3}(2\alpha_V + 1)g_{O8}^V \ , \nu_1$$

$$g_{\Sigma\omega} = 2\alpha_V g_{O8}^V \ , \qquad g_{\Sigma\phi} = -\sqrt{2}(2\alpha_V - 1)g_{O8}^V \ , \nu_1$$

$$g_{\Xi\omega} = (2\alpha_V - 1)g_{O8}^V \ , \qquad g_{\Xi\phi} = -2\sqrt{2}\alpha_V g_{O8}^V \ .$$

In the limit $\alpha_V = 1$, the relative values of the coupling constants are related to the additive quark model via:

$$g_{\Lambda\omega} = g_{\Sigma\omega} = 2g_{\Xi\omega} = \frac{2}{3}g_{N\omega} = 2g_{O8}^V \ , \qquad g_{\Lambda\phi} = g_{\Sigma\phi} = \frac{g_{\Xi\phi}}{2} = \frac{\sqrt{2}}{3}g_{N\omega} \ .$$

Note that all coupling constants are fixed once e.g. $g_{N\omega}$ is specified.

For the coupling of the baryon resonances to the vector mesons we obtain the same Clebsch-Gordan coefficients as for the coupling to the scalar mesons. This leads to the following relations between the coupling constants:

$$g_{\Delta\omega} = (3 - \alpha_{DV})g_{DV} \ , \qquad g_{\Delta\phi} = \sqrt{2}\alpha_{DV}g_{DV} \ ,$$

$$g_{\Sigma^*\omega} = 2g_{DV} \ , \qquad g_{\Sigma^*\phi} = \sqrt{2}g_{DV} \ ,$$

$$g_{\Xi^*\omega} = (1 + \alpha_{DV})g_{DV} \ , \qquad g_{\Xi^*\phi} = \sqrt{2}(2 - \alpha_{DV})g_{DV} \ ,$$

$$g_{\Omega\omega} = \alpha_{DV}g_{Rv} \ , \qquad g_{\Omega\phi} = \sqrt{2}(3 - \alpha_{DV})g_{DV} \ .$$

To obtain the coupling of the baryon decuplet to the spin–1 mesons we set $\alpha_R = 0$, since the strange vector meson ϕ should not couple to the Δ baryon, in analogy to the octet case. The resulting coupling constants again obey the additive quark model constraints:

$$g_{\Delta\omega} = \frac{3}{2}g_{\Sigma^*\omega} = 3g_{\Xi^*\omega} = 3g_{DV} \ , \qquad g_{\Omega\omega} = 0 \ , \nu_1 \tag{31}$$

$$g_{\Omega\phi} = \frac{3}{2}g_{\Xi^*\phi} = 3g_{\Sigma^*\phi} = \sqrt{2}g_{\Delta\omega} \ , \qquad g_{\Delta\phi} = 0 \ . \tag{32}$$

This means that in the case of the baryon decuplet all coupling constants are again fixed if the overall coupling g_{DV} is specified. Since there is not a vacuum restriction on the Δ-ω coupling like in the case of the scalar mesons, we have to consider different constraints. This will be discussed in Sec. 9.

5.3   Vector meson masses

Here we discuss the mass terms of the vector mesons. The simplest scale-invariant form

$$\mathcal{L}_{\text{vec}}^{(1)} = \frac{1}{2}m_V^2 \frac{\chi^2}{\chi_0^2}\text{Tr}V_\mu V^\mu + 2g_4^4\text{Tr}(V_\mu V^\mu)^2 \,, \tag{33}$$

implies a mass degeneracy for the meson nonet. The first term of (33) is made scale invariant by multiplying it with an appropriate power of the glueball field χ (see Sec. 5.5 for details). To split the masses, one can add the chiral invariant [25,26]

$$\mathcal{L}_{\text{vec}}^{(2)} = \frac{1}{4}\mu\text{Tr}\left[V_{\mu\nu}V^{\mu\nu}X^2\right] \,. \tag{34}$$

A detailed description can be found in [15]. The axial vector meson masses can be described by adding terms analogous to (34). We refrain from discussing them further, see [25,27].

5.4   Scalar mesons

The nonlinear realization of chiral symmetry offers many more possibilities to form chiral invariants: the couplings of scalar mesons with each other are only governed by $SU(3)_V$-symmetry. However, only three kinds of independent invariants exist, namely

$$I_1 = \text{Tr}X \,, \quad I_2 = \text{Tr}X^2 \,, \quad I_3 = \det X \,. \tag{35}$$

All other invariants, $\text{Tr}X^n$, with $n \geq 3$, can be expressed as a function of the invariants shown in (35), see [15]. For our calculations, the invariants of (35) are considered as building blocks, from which the different forms of the meson-meson interaction can be constructed. In this report we will only discuss the potential of the $SU(3)$ linear σ-model [28]. The connection to the models [5,29] and [2–4] is discussed in detail in [15].

The concept of broken scale invariance leading to the trace anomaly in (massless) QCD, $\theta^\mu_\mu = (\beta_{\rm QCD}/(2g))\mathcal{G}^a_{\mu\nu}\mathcal{G}^{\mu\nu}_a$ ($\mathcal{G}_{\mu\nu}$ is the gluon field strength tensor of QCD), can be mimicked in an effective Lagrangian at tree level [10] through the introduction of the potential

$$\mathcal{L}_{\rm scale} = -k_4\chi^4 - \frac{1}{4}\chi^4 \ln\frac{\chi^4}{\chi^4_0} + \frac{\delta}{3}\chi^4 \ln\frac{I_3}{\det\langle X\rangle} \, . \tag{36}$$

The effect [1] of the logarithmic term $\sim \chi^4 \ln\chi$ is to break the scale invariance. This leads to the proportionality $\theta^\mu_\mu \sim \chi^4$, as can be seen from

$$\theta^\mu_\mu = 4\mathcal{L} - \chi\frac{\partial\mathcal{L}}{\partial\chi} - 2\partial_\mu\chi\frac{\partial\mathcal{L}}{\partial(\partial_\mu\chi)} = \chi^4 \, , \tag{37}$$

which is a consequence of the definition of the scale transformations [30]. This holds only, if the meson-meson potential is scale invariant, which can be achieved by multiplying the invariants of scale dimension less than four with an appropriate power of the dilaton field χ.

The comparison of the trace anomaly of QCD with that of the effective theory allows for the identification of the χ-field with the gluon condensate:

$$\theta^\mu_\mu = \left\langle \frac{\beta_{\rm QCD}}{2g}\mathcal{G}^a_{\mu\nu}\mathcal{G}^{\mu\nu}_a \right\rangle \equiv (1-\delta)\chi^4 \, . \tag{38}$$

The parameter δ originates from the second logarithmic term with the chiral invariant I_3 (see also [5] for the chiral SU(2) linear σ-model). An orientation for the value of δ may be taken from $\beta_{\rm QCD}$ at the one loop level, with N_c colors and N_f flavors,

$$\beta_{\rm QCD} = -\frac{11N_cg^3}{48\pi^2}\left(1 - \frac{2N_f}{11N_c}\right) + \mathcal{O}(g^5) \, . \tag{39}$$

Here the first number in parentheses arises from the (antiscreening) self-interaction of the gluons and the second term, proportional to N_f, is the (screening) contribution of quark pairs. Equation (39) suggests the value

---

[1] According to [10], the argument of the logarithm has to be chirally and parity invariant. This is fulfilled by the dilaton, χ, which is both a chiral singlet as well as a scalar.

$\delta = 2/11$ for three flavors and three colors. This value gives the order of magnitude about which the parameter δ will be varied.

For simplicity, we will also consider the case in which $\chi = \chi_0$, where the gluon condensate does not vary with density. We will refer to this case as the *frozen glueball limit*.

5.6 Explicitly broken chiral symmetry

In order to eliminate the Goldstone modes from a chiral effective theory, explicit symmetry breaking terms have to be introduced. Here, we use

$$\mathcal{L}_{\text{SB}} = -\frac{1}{2}m_{\eta_0}^2 \text{Tr}Y^2 - \frac{1}{2}\text{Tr}A_p\left(uXu + u^\dagger X u^\dagger\right) - \text{Tr}\left(A_s - A_p\right)X \ . \tag{40}$$

The first term, which breaks the $U(1)_A$ symmetry, gives a mass to the pseudoscalar singlet. The second term is motivated by the explicit symmetry breaking term of the linear σ-model,

$$\frac{1}{2}\text{Tr}A_p(M + M^\dagger) = \text{Tr}A_p\left(u(X + iY)u + u^\dagger(X - iY)u^\dagger\right) \ , \tag{41}$$

with $A_p = 1/\sqrt{2}\text{diag}(m_\pi^2 f_\pi, m_\pi^2 f_\pi, 2m_K^2 f_K - m_\pi^2 f_\pi)$ and $m_\pi = 139$ MeV, $m_K = 498$ MeV. Inserting the spin-0 meson matrix one obtains

$$-\mathcal{L}_{\text{SB}} = \frac{\chi^2}{\chi_0^2}\left(m_\pi^2 f_\pi \sigma + (\sqrt{2}m_K^2 f_K - \frac{1}{\sqrt{2}}m_\pi^2 f_\pi)\zeta\right) \ . \tag{42}$$

From this the VEV of σ and ζ are fixed by the PCAC relations for the π- and K-mesons.

$$\sigma_0 = -f_\pi \qquad \zeta_0 = \frac{1}{\sqrt{2}}(f_\pi - 2f_K) \ . \tag{43}$$

For simplicity, η_0/η_8 mixing is neglected through omitting Y from the second term of equation (40). If this term is included, we get a mixing angle of $\theta = 16°$ for parameter set C_1 [15], which agrees well with experiment, $\theta_{\text{exp}} \approx 20°$ from $\eta, \eta' \to \gamma\gamma$.

In the case of $SU(3)_V$-symmetry, the quadratic Gell-Mann Okubo mass formula, $3m_{\eta_8}^2 + m_\pi^2 - 4m_K^2 = 0$, is satisfied.

The third term breaks $SU(3)_V$-symmetry. $A_s = \text{diag}(x, x, y)$ can be used to remove the vacuum constraints on the parameters of the meson-meson potential by adjusting x and y in such a way that the terms linear in σ and ζ vanish in the vacuum.

6 Mean-field approximation

The terms discussed so far involve the full quantum operator fields which cannot be treated exactly. To investigate hadronic matter properties at finite baryon density we adopt the mean-field approximation. This is a nonperturbative relativistic method to solve approximately the nuclear many body problem by replacing the quantum field operators by its classical expectation values (for a recent review see [31]), i.e. the fluctuations around constant vacuum expectation values of the field operators are neglected:

$$\sigma(x) = \langle\sigma\rangle + \delta\sigma \to \langle\sigma\rangle \equiv \sigma \,, \quad \zeta(x) = \langle\zeta\rangle + \delta\zeta \to \langle\zeta\rangle \equiv \zeta \,,$$
$$\omega_\mu(x) = \langle\omega\rangle\delta_{0\mu} + \delta\omega_\mu \to \langle\omega_0\rangle \equiv \omega \,,$$
$$\phi_\mu(x) = \langle\phi\rangle\delta_{0\mu} + \delta\phi_\mu \to \langle\phi_0\rangle \equiv \phi \,.$$

The fermions are treated as quantum mechanical one-particle operators. The derivative terms can be neglected and only the time-like component of the vector mesons $\omega \equiv \langle\omega_0\rangle$ and $\phi \equiv \langle\phi_0\rangle$ survive if we assume homogeneous and isotropic infinite baryonic matter. Additionally, due to parity conservation we have $\langle\pi_i\rangle = 0$. After performing these approximations, the Lagrangian (26) becomes

$$\mathcal{L}_{BM} + \mathcal{L}_{BV} = -\sum_i \overline{\psi_i}[g_{i\omega}\gamma_0\omega^0 + g_{i\phi}\gamma_0\phi^0 + m_i^*]\psi_i \,,$$

$$\mathcal{L}_{\text{vec}} = \frac{1}{2}m_\omega^2\frac{\chi^2}{\chi_0^2}\omega^2 + \frac{1}{2}m_\phi^2\frac{\chi^2}{\chi_0^2}\phi^2 + g_4^4(\omega^4 + 2\phi^4) \,,$$

$$\mathcal{V}_0 = \frac{1}{2}k_0\chi^2(\sigma^2 + \zeta^2) - k_1(\sigma^2 + \zeta^2)^2 - k_2\left(\frac{\sigma^4}{2} + \zeta^4\right)$$
$$\qquad - k_3\chi\sigma^2\zeta + k_4\chi^4 + \frac{1}{4}\chi^4\ln\frac{\chi^4}{\chi_0^4} - \frac{\delta}{3}\ln\frac{\sigma^2\zeta}{\sigma_0^2\zeta_0} \,,$$

$$\mathcal{V}_{\text{SB}} = \left(\frac{\chi}{\chi_0}\right)^2\left[m_\pi^2 f_\pi\sigma + \left(\sqrt{2}m_K^2 f_K - \frac{1}{\sqrt{2}}m_\pi^2 f_\pi\right)\zeta\right] \,,$$

with the effective mass of the baryon i, which is defined according to Sec. 5.1 and $i = N, \Lambda, \Sigma, \Xi, \Delta, \Sigma^*, \Xi^*, \Omega$.

Now it is straightforward to write down the expression for the thermodynam-

ical potential of the grand canonical ensemble Ω per volume V at a given chemical potential μ and zero temperature:

$$\frac{\Omega}{V} = -\mathcal{L}_{\text{vec}} - \mathcal{L}_0 - \mathcal{L}_{\text{SB}} - \mathcal{V}_{\text{vac}} - \sum_i \frac{\gamma_i}{(2\pi)^3} \int d^3k [E_i^*(k) - \mu_i^*] . \tag{44}$$

The vacuum energy $\mathcal{V}_{\text{vac}}$ (the potential at $\rho = 0$) has been subtracted in order to get a vanishing vacuum energy. γ_i denote the fermionic spin-isospin degeneracy factors. The single particle energies are $E_i^*(k) = \sqrt{k_i^2 + m_i^{*2}}$ and the effective chemical potentials read $\mu_i^* = \mu_i - g_{\omega i}\omega - g_{\phi i}\phi$.

The mesonic fields are determined by extremizing $\frac{\Omega}{V}(\mu, T = 0)$:

$$\frac{\partial(\Omega/V)}{\partial\chi} = -\omega^2 m_\omega^2 \frac{\chi}{\chi_0^2} + k_0\chi(\sigma^2 + \zeta^2) - k_3\sigma^2\zeta\nu_1 \tag{45}$$

$$+ \left(4k_4 + 1 + 4\ln\frac{\chi}{\chi_0} - 4\frac{\delta}{3}\ln\frac{\sigma^2\zeta}{\sigma_0^2\zeta_0}\right)\chi^3\nu_1 \tag{46}$$

$$+2\frac{\chi}{\chi_0^2}\left[m_\pi^2 f_\pi\sigma + (\sqrt{2}m_K^2 f_K - \frac{1}{\sqrt{2}}m_\pi^2 f_\pi)\zeta\right] = 0 , \tag{47}$$

$$\frac{\partial(\Omega/V)}{\partial\sigma} = k_0\chi^2\sigma - 4k_1(\sigma^2 + \zeta^2)\sigma - 2k_2\sigma^3 - 2k_3\chi\sigma\zeta - 2\frac{\delta\chi^4}{3\sigma} \tag{48}$$

$$\nu_1 + \left(\frac{\chi}{\chi_0}\right)^2 m_\pi^2 f_\pi + \sum_i \frac{\partial m_i^*}{\partial\sigma}\rho_i^s = 0 , \tag{49}$$

$$\frac{\partial(\Omega/V)}{\partial\zeta} = k_0\chi^2\zeta - 4k_1(\sigma^2 + \zeta^2)\zeta - 4k_2\zeta^3 - k_3\chi\sigma^2 - \frac{\delta\chi^4}{3\zeta}\nu_1 \tag{50}$$

$$+ \left(\frac{\chi}{\chi_0}\right)^2\left[\sqrt{2}m_K^2 f_K - \frac{1}{\sqrt{2}}m_\pi^2 f_\pi\right] + \sum_i \frac{\partial m_i^*}{\partial\zeta}\rho_i^s = 0 , \tag{51}$$

$$\frac{\partial(\Omega/V)}{\partial\omega} = -\left(\frac{\chi}{\chi_0}\right) m_\omega^2\omega - 4g_4^4\omega^3 + \sum_i \frac{g_{i\omega}}{\rho_i} = 0 , \tag{52}$$

$$\frac{\partial(\Omega/V)}{\partial\phi} = -\left(\frac{\chi}{\chi_0}\right) m_\phi^2\phi - 8g_4^4\phi^3 + \sum_i \frac{g_{i\phi}}{\rho_i} = 0 . \tag{53}$$

The scalar densities ρ_i^s and the vector densities ρ_i can be calculated analytically for the case $T = 0$, yielding

$$\rho_i^s = \gamma_i \int \frac{d^3k}{(2\pi)^3}\frac{m_i^*}{E_i^*} = \frac{\gamma_i m_i^*}{4\pi^2}\left[k_{Fi}E_{Fi}^* - m_i^{*2}\ln\left(\frac{k_{Fi} + E_{Fi}^*}{m_i^*}\right)\right] , \tag{54}$$

$$\rho_i = \gamma_i \int_0^{k_{Fi}} \frac{d^3k}{(2\pi)^3} = \frac{\gamma_i k_{Fi}^3}{6\pi^2} . \tag{55}$$

The energy density and the pressure follow from the Gibbs–Duhem relation, $\epsilon = \Omega/V + \mu_i \rho^i$ and $p = -\Omega/V$. Applying the Hugenholtz–van Hove theorem [32], the Fermi surfaces are given by $E^*(k_{Fi}) = \sqrt{k_{Fi}^2 + m_i^{*2}} = \mu_i^*$.

7 Nuclear matter

Here we discuss how the parameters of the effective model are fixed to vacuum and nuclear matter ground state properties. Furthermore predicted observables will be discussed.

7.1 Fixing of parameters

The elements of the matrix A_p are fixed to fulfill the PCAC-relations of the pion and the kaon, respectively. Therefore, the parameters of the chirally invariant potential, k_0 and k_2, are used to ensure an extremum in the vacuum. As for the remaining constants, k_3 is constrained by the η'-mass, and k_1 is varied to give a σ-mass of the order of $m_\sigma = 500$ MeV. The VEV of the gluon condensate, χ_0, is fixed to fit the binding energy of nuclear matter $\epsilon_0/\rho - m_N = -16$ MeV at the saturation density $\rho_0 = 0.15\,\mathrm{fm}^{-3}$. The VEV of the fields σ_0 and ζ_0 are constrained by the decay constants of the pion and the kaon, respectively, see (43). As stated before the coupling constant of the baryons to the scalar mesons are fitted to the experimental values of their vacuum masses. The coupling constant of the spin-1 mesons to the spin-$\frac{1}{2}$ baryons is chosen to ensure that the nuclear matter ground state pressure vanishes. The coupling of the baryon resonances to the spin-1 mesons will be discussed in (9).

7.2 Vacuum and nuclear matter properties

We will mainly concentrate on the results obtained using three different parameter sets:

- C_1: frozen glueball, baryon masses without additional symmetry breaking
- C_2: frozen glueball, baryon masses including additional symmetry breaking
- C_3: non-frozen glueball, baryon masses like C_1

The values of the parameters can be seen in Table 4.

The hadronic masses in the vacuum have reasonable values for all fits (Table 2 and 3).

Table 4
Parameters of the fits (see text)

	k_0	k_1	k_2	k_3	k_{3m}	k_4	33δ
C_1	2.37	1.40	-5.55	-2.65	0	-.23	2
C_2	2.36	1.40	-5.55	-2.64	0	-.23	2
C_3	2.35	1.40	-5.55	-2.60	0	-.23	2

According to Table 3, the values of the effective nucleon mass and the compressibility in the medium (at ρ_0) are reasonable. To obtain these values the inclusion of a quartic term for vector mesons (see (33)) was necessary. Table 3 shows the nucleon and Lambda potential in saturated nuclear matter, which are in good agreement with extrapolations from binding energies in nuclei. Using different forms for the mesonic potential one can obtain other successful models for the description of nuclear matter and finite nuclei. This has been done for the Minnesota model [5] and the Walecka model in [15].

8 Nuclei, Hypernuclei

As was pointed out in [33], reproducing the nuclear matter equilibrium point is not sufficient to ensure a quantitative description of nuclear phenomenology. For this, one has to study the systematics of finite nuclei. To apply the model to the description of finite nuclei, we also adopt the mean-field approximation. Compared to nuclear matter one has to take additional terms into account for the description of finite nuclei.

- since one considers now finite system, the spatial derivatives of the fields have to be taken into account
- since the system is not isospin symmetric anymore, the expectation value for the ρ-meson does not vanish anymore
- electromagnetic interactions have to be taken into account

This leads to the following additional terms for the Lagrangian:

$$\mathcal{L}'_{\text{kin}} = -i\overline{N}\gamma_i\nabla^i N - \frac{1}{2}\sum_{\varphi=\sigma,\zeta,\chi,\omega,\rho,A}\nabla_i\varphi\nabla^i\varphi \,,\nu_1 \tag{56}$$

$$\mathcal{L}'_{BV} = -\overline{N}\gamma_0\left[g_{N\rho}\tau_3\rho_0 + \frac{1}{2}e(1+\tau_3)A_0\right]N\nu_1 \,, \tag{57}$$

$$\mathcal{L}'_{\text{vec}} = \frac{1}{2}\frac{\chi^2}{\chi_0^2}m_\rho^2\rho^2 + g_4^4\left(6\omega^2\rho^2 + \rho^4\right) \,. \tag{58}$$

Table 5

Bulk properties of nuclei: Prediction (left) and experimental values (right) for binding energy E/A, charge radius r_{ch}, and spin-orbit splitting of Oxygen (^{16}O with $\delta p \equiv p_{3/2} - p_{1/2}$), Calcium (^{40}Ca with $\delta d \equiv d_{5/2} - d_{3/2}$) and Lead (^{208}Pb with $\delta d \equiv 2d_{5/2} - 2d_{3/2}$)

	^{16}O			^{40}Ca			^{208}Pb		
	E/A	r_{ch}	δp	E/A	r_{ch}	δd	E/A	r_{ch}	δd
Exp.	-7.98	2.73	5.5-6.6	-8.55	3.48	5.4-8.0	-7.86	5.50	0.9-1.9
C_1	-7.30	2.65	6.05	-7.98	3.42	6.19	-7.56	5.49	1.59
C_2	-7.40	2.65	5.21	-8.07	3.42	5.39	-7.61	5.50	1.41
C_3	-7.29	2.65	6.06	-7.98	3.42	6.22	-7.54	5.49	1.61
M_1	-7.19	2.68	5.60	-7.93	3.45	5.83	-7.56	5.53	1.53
M_2	-7.34	2.67	5.90	-8.03	3.44	6.08	-7.61	5.52	1.58
W_1	-8.28	2.63	5.83	-8.63	3.42	5.91	-7.71	5.51	1.43
W_2	-8.23	2.63	5.84	-8.60	3.42	5.94	-7.75	5.51	1.45
W_3	-7.98	2.67	5.23	-8.47	3.44	5.45	-7.72	5.55	1.33

The resulting Dirac equation for the nucleon and the equation for the photon field are of the form given, e.g. by Reinhard [34]. The densities $\rho_s = \langle \overline{N}N \rangle$, $\rho_B = \langle \overline{N}\gamma_0 N \rangle$, $\rho_3 = \langle \overline{N}\gamma_0 \tau_3 N \rangle$ can be expressed in terms of the components of the nucleon Dirac spinors in the usual way [31]. The set of coupled equations is solved numerically in an accelerated gradient iteration following [35]. Without changing the parameters of the model, the properties of nuclei can readily be predicted.

The charge densities of ^{16}O, ^{40}Ca and ^{208}Pb are quite close to experiment. They exhibit relatively small radial oscillations (Figs. 1, 2, and 3), though such oscillations are not seen in the experimental data[2]. The experimental charge densities are from [37], where a three-parameter Fermi model was used[3]. The charge radii are close to the experimental values. Figure 4 shows the charge form factor of ^{208}Pb for parameter set C_1 in momentum space. For small momenta the agreement with experiment [37] is very good, only for larger momenta deviations are observable but at the same scale as in the nonlinear Walecka model [29]. The binding energies of ^{16}O, ^{40}Ca and ^{208}Pb are in reasonable agreement with the experimental data (see Table 5). Nevertheless they are off by approximately 0.5 MeV. To correct this, a direct fit to nuclear

[2] Similar problems exist also for nonchiral models, for a discussion see [33,36]

[3] A more sophisticated model-independent analysis by means of an expansion for the charge distribution as a sum of Gaussians would lead to an even closer correspondence between our results and the experimental data.
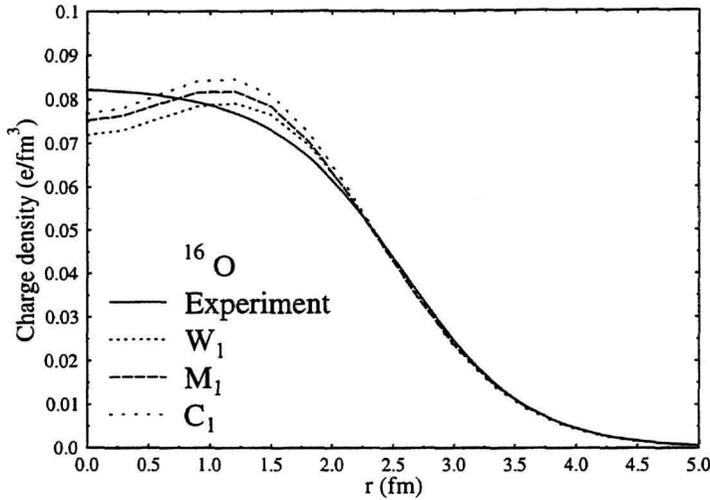
Fig. 1. Charge density for ^{16}O for the parameter sets indicated in [15]. (C) chiral $SU(3)$ model. (M) chiral $SU(2)$ Minnesota model. (W) extended Walecka model. The experimental charge density is parameterized with a three-parameter Fermi model [37]
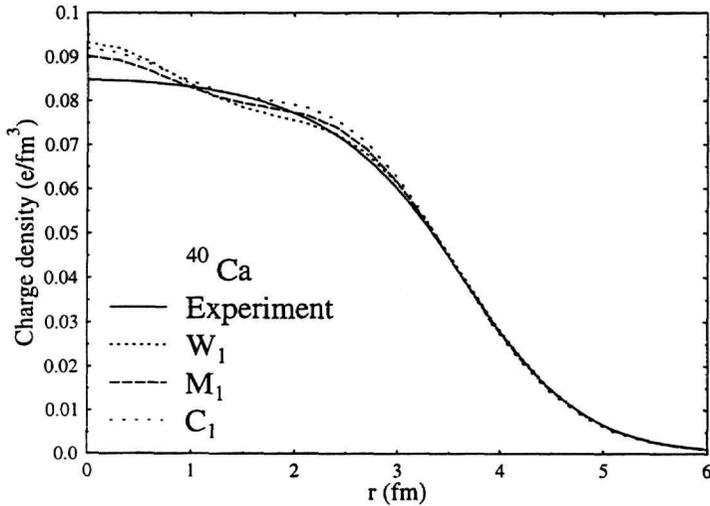

Fig. 2. As for Fig. 1, but for ^{40}C

properties has to be done [38].

As can be seen from Table 5, models C_1 and C_2 exhibit a spin-orbit split-ting that lies within the band of the experimental uncertainty given in [39]. The single-particle energies of ^{208}Pb are close to those of the Walecka model extended to include nonlinear σ^3 and σ^4 terms [4] or the model [5], both for neutrons (Fig. 5) and for protons (Fig. 6). This is encouraging since neither the nucleon/scalar meson nor the nucleon/ρ meson coupling constants can be
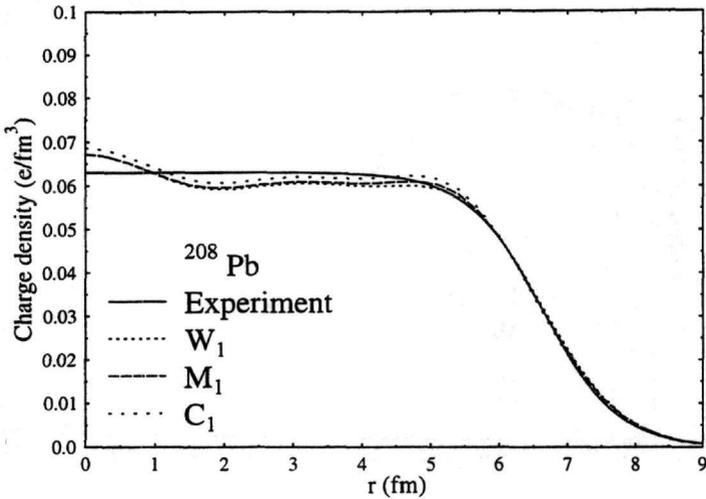
Fig. 3. As for Fig. 1, but for ^{208}Pb
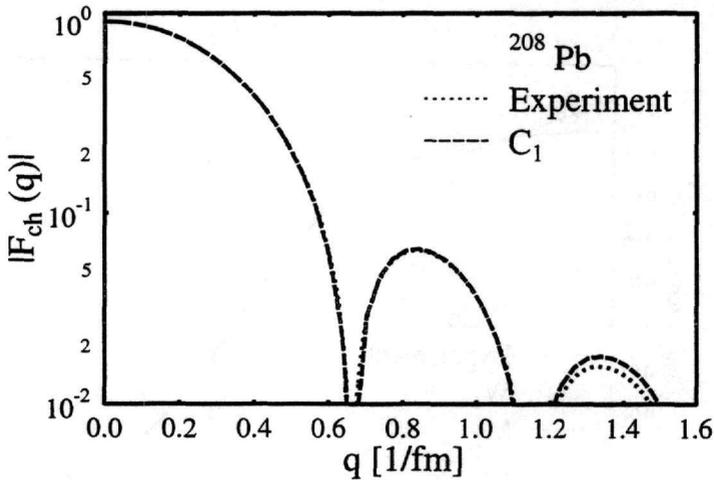
Fig. 4. Charge form factor for ^{208}Pb

adjusted to nuclear matter or nuclear properties, in contrast to the Walecka model [4]. Figure 7 shows the binding energy per nucleon, the two nucleon separation energy and the two-nucleon gap for a nucleus with 126 neutrons and different numbers of protons (left) as well as a nucleus with 82 protons and varying numbers of neutrons. One perceives that the model fitted to infinite nuclear matter properties correctly predicts ^{208}Pb to be a doubly magic nucleus. All these results show that a satisfactory description of finite nuclei is possible within the chiral $SU(3)$ model fitted to nuclear matter properties. Fits to properties of finite nuclei promise to yield even better results [38].
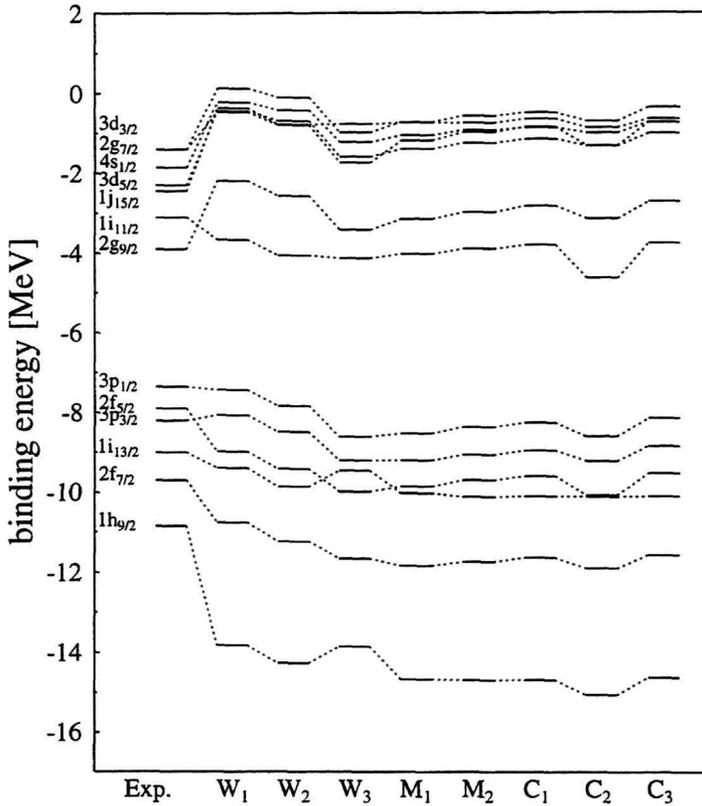
Fig. 5. Single particle energies of neutrons near the Fermi energy in ^{208}Pb. Experimentally measured levels are compared with predictions from various potentials

8.1 Superheavy nuclei

Starting from the well-known magic proton and neutron numbers, the question for the next, so far unknown, magic numbers is very important. According to [40] most relativistic mean field models find the doubly magic nuclei for $Z = 120$, $N = 172$ and some predict a doubly magic nuclei with $N = 184$ and $Z = 120$. Fig. 8 shows the binding energy per particle, the two-nucleon separation energy and the two-nucleon gap around N=172 and Z=120. The chiral $SU(3)$ model predicts Z=114 as a shell closure for a neutron number of 172. One detects a peak at a proton number of 120 as well, but this nucleus is beyond the drip line. Figure 9 shows the same observables like Fig. 8 but for N=184 (left) and Z=120 (right). One recognizes two possible magic numbers in that region for protons, namely Z=114 and Z=120. The neutron shell closures are N=172, N=184 and N=198. These results should only be seen as preliminary, since on the one hand an improved fitting to doubly magic nuclei and on the other hand the usage of other pair interactions than constant gap pairing

193
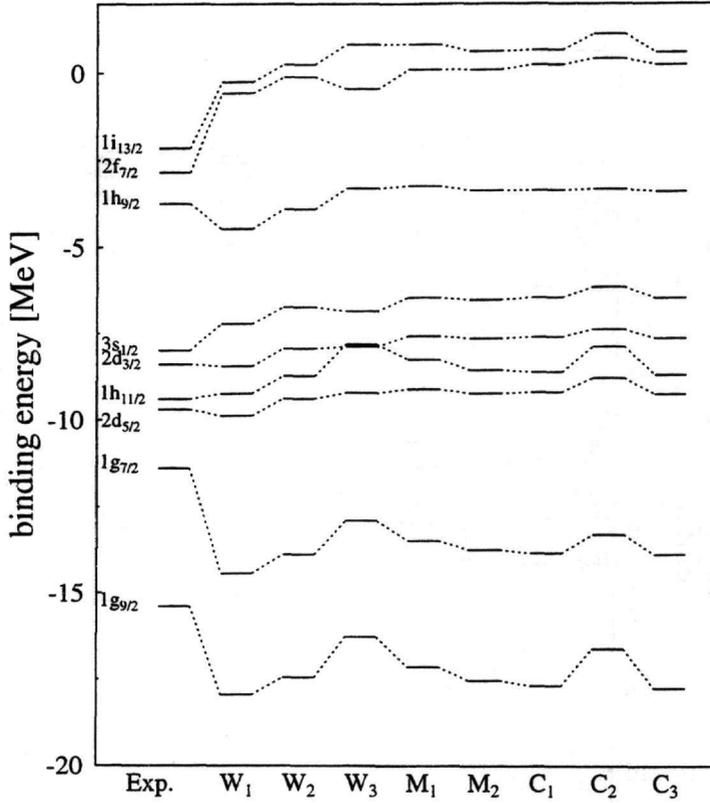
Fig. 6. As for Fig. 5, but for protons

should yield better results.

8.2 Hypernuclei

We want to compare the experimental hypernuclear data with the results obtained using parameter set C_1. Table 6 shows the experimental $\Lambda - n$-hole one-particle-energy differences for the nuclei $^{12}_{\Lambda}C$, $^{16}_{\Lambda}O$ and $^{40}_{\Lambda}Ca$ from [41,42]. These values are compared to the results from the chiral $SU(3)$ model using parameter set C_1. One can see that the deviations in the most cases are smaller than experimental errors. This is even more remarkable, since the coupling constants $g_{\Lambda\sigma}$ and $g_{\Lambda\omega}$ have not been fitted to any hypernuclear data. But the inclusion of an explicitly symmetry breaking term was necessary to fix the potential depth of a Λ-particle in infinite nuclear matter to $U_\Lambda = -28\text{MeV}$. Table 6 also shows the results for a Walecka model that was extended to the strange sector [35]. This model yields even better agreement with experiment, but here the coupling constants of the Λ were fitted to hypernuclear data. Figure 10 shows energy levels of Λ-hyperons in various nuclei, as a function
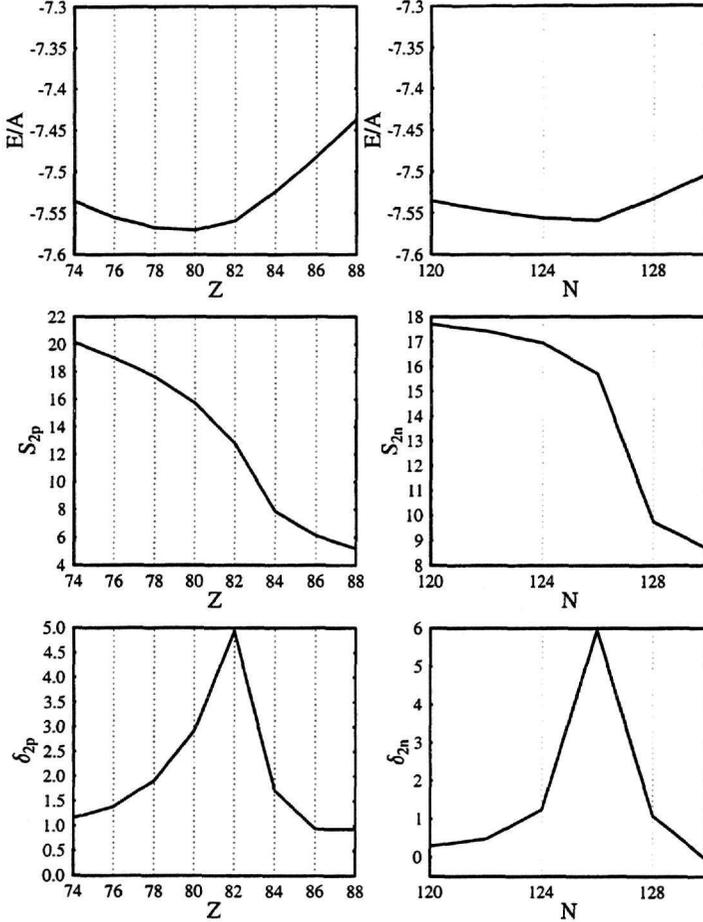
Fig. 7. Shell closures around ^{208}Pb. (**Top**) Energy per particle, (**middle**) two-nucleon separation energy and (**bottom**) two-nucleon gap for different isotones with (**left**) N=126 and (**right**) Z=82

of $A^{-\frac{2}{3}}$ and these are compared to calculated Λ one-particle levels for nuclei with $A-1$ nucleons. It can be seen that the results agree well with the experimental data. Furthermore it can be seen, that all levels converge to the point 28MeV for increasing A. From this extrapolation the potential depth of the Λ in nuclear matter was first deduced [43]. As a further application of the chiral $SU(3)$ model in the strange sector Fig. 11 shows the binding energy of baryons in nuclei with different numbers of Λ hyperons. It can be seen that with increasing number of Λ's, the binding energy first decreases and then rises again. That is not astonishing, since with adding hyperons a new degree of freedom is introduced. The Λ's are deeper bound than the lowest bound nucleons.
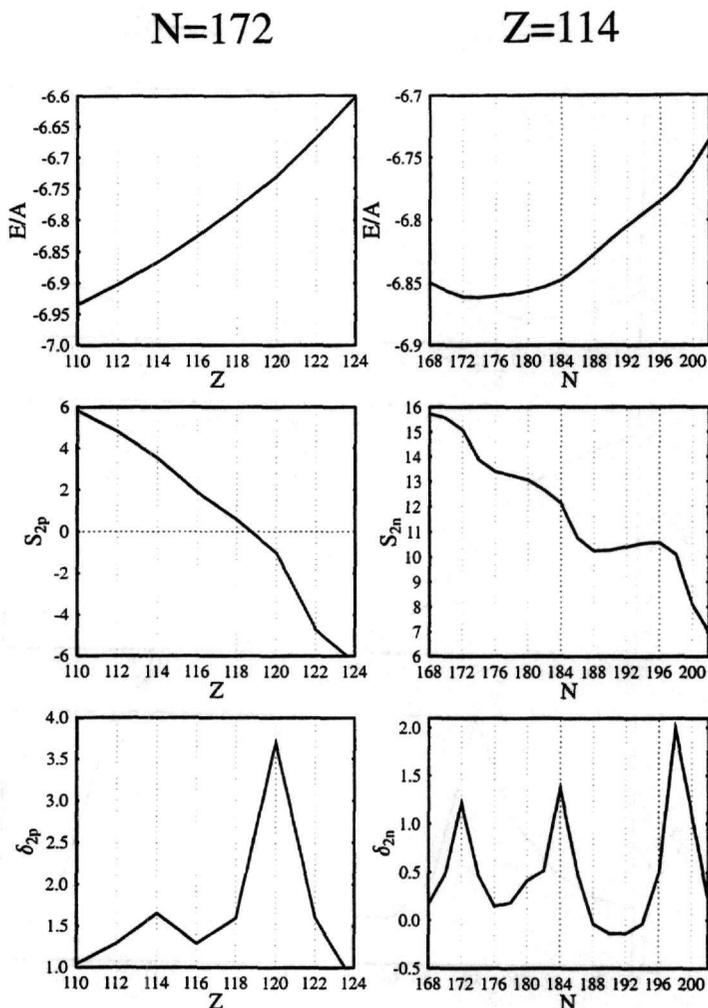
Fig. 8. Superheavy nuclei with Z=114 and N=172. Same observables as in 7

9 Hadronic matter at high temperature and density

9.1 Extrapolation to higher densities

Once the parameters have been fixed to nuclear matter at ρ_0 the condensates and hadron masses at high baryon densities can be investigated.

In Fig. 12 we display the scalar mean fields σ, ζ and χ as a function of the baryon density for vanishing strangeness using parameter set C_3. One sees that the gluon condensate χ stays nearly constant when the density increases, implying that the approximation of a frozen glueball is reasonable. The strange condensate ζ is only reduced by about 10 percent from its vacuum expecta-
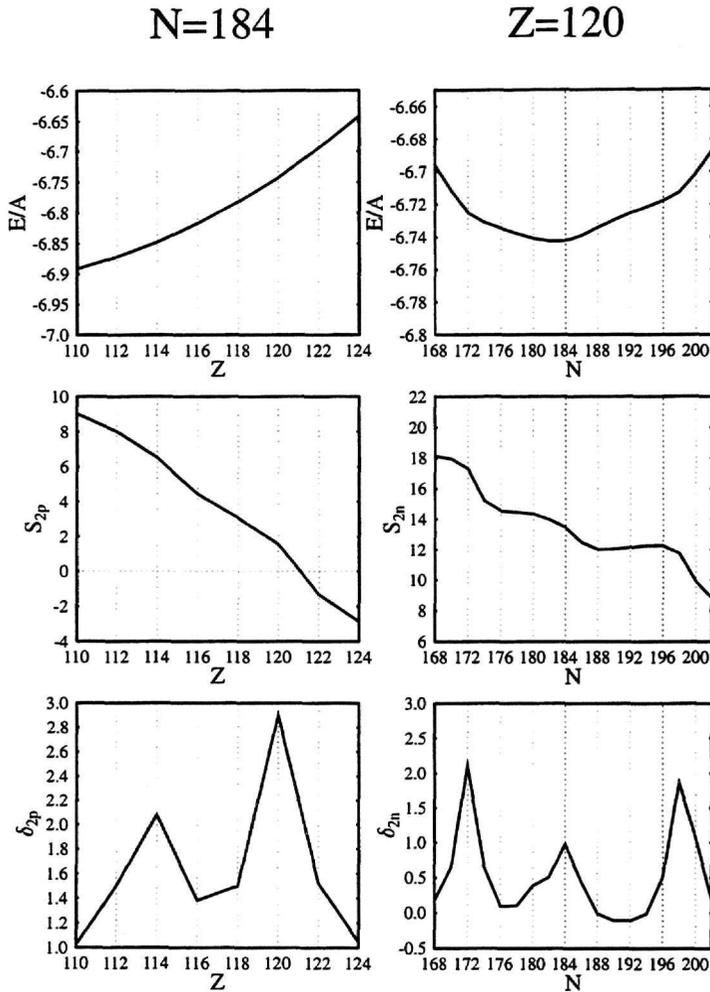
Fig. 9. Superheavy nuclei with Z=120 and N=184. Same observables as in 7

tion value. This is not surprising since there are only nucleons in the system and the nucleon–ζ coupling is fairly weak. The main effect occurs for the non–strange condensate σ. The field has dropped to 30% of its vacuum expectation value at 4 times normal nuclear density. If we extrapolate to even higher densities one observes that the σ field does not change significantly, that means all fields saturate around 4 ρ_0 Since the baryon masses are generated by the condensates σ and ζ, the change of these scalar fields causes the change of the baryon masses in medium. The density dependence of the effective spin-$\frac{1}{2}$ baryon masses is shown for C_1 in Fig. 13. When the density in the system increases, the masses drop significantly up to 4 times normal nuclear density. This corresponds to the above mentioned behavior of the condensates. Furthermore, one observes that the change of the baryon mass depends on the strange quark content of the baryon. This is caused by the different coupling

Table 6
Experimental Λ-n-hole one-particle-energy-gaps of the nuclei $^{12}_{\Lambda}$C, $^{16}_{\Lambda}$O and $^{40}_{\Lambda}$Ca compared to calculations in the Walecka model [35] and parameter set C_1 of the chiral $SU(3)$-model. The experimental data was obtained from excitation spectra from [41,42]

		Experiment		Walecka model		C_1 prediction	
Kern	Niveaus	E	ΔE	E	ΔE	E	ΔE
$^{12}_{\Lambda}$C	$(1s_{1/2}, 1p_{3/2}^{-1})_{\Lambda n}$	6.72	2	5.02	1.70	7.76	-1.04
	$(1p_{3/2}, 1p_{3/2}^{-1})_{\Lambda n}$	18.48	2	17.21	1.27	15.78	2.7
$^{16}_{\Lambda}$O	$(1p_{3/2}, 1p_{3/2}^{-1})_{\Lambda n}$	19.20	2	18.88	0.32	19.29	-0.09
	$(1p_{1/2}, 1p_{1/2}^{-1})_{\Lambda n}$	13.20	2	13.89	-0.69	14.36	-1.16
	$(1s_{1/2}, 1p_{3/2}^{-1})_{\Lambda n}$	9.90	2	9.46	0.44	11.28	-1.38
	$(1s_{1/2}, 1p_{1/2}^{-1})_{\Lambda n}$	3.35	2	3.53	-0.18	5.16	-1.81
$^{40}_{\Lambda}$Ca	$(1p_{1/2}, 1d_{3/2}^{-1})_{\Lambda n}$	5.79	2	7.40	-1.61	8.14	-2.35
	$(1d_{3/2}, 1d_{3/2}^{-1})_{\Lambda n}$	14.47	2	15.48	-1.01	15.58	-1.11
	$(1d_{5/2}, 1d_{5/2}^{-1})_{\Lambda n}$	19.35	2	20.71	-1.36	20.31	-0.96
	$(1f_{7/2}, 1d_{5/2}^{-1})_{\Lambda n}$	28.24	2	27.14	1.10	26.49	1.75
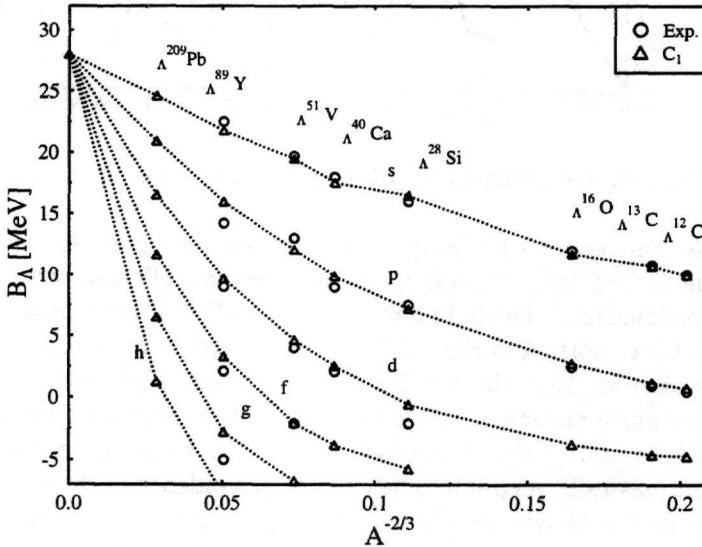
Fig. 10. Energy levels of Λ-hypernuclei as a function of $A^{-\frac{2}{3}}$ compared to experiment [43]. The energy levels converge to the value -28MeV for the potential depth of the Λ in nuclear matter
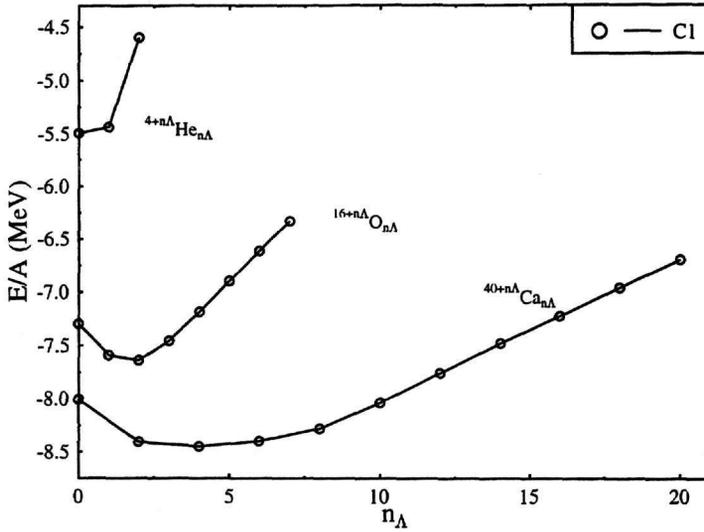
Fig. 11. Binding energy for multi-Λ hypernuclei

of the baryons to the non-strange and strange condensate. Figure 14 shows the masses of the vector mesons. They are predicted to stay nearly constant if the density increases. As a further approximation we show in Fig. 15 the nucleon and anti-nucleon potentials as a function of density . Here one can see the very important influence of the quartic vector meson self-interaction. Including this term, the anti-nucleons become overcritical at densities around $12\rho_0$. If the ω^4 term is neglected anti-nucleons already become critical for $\rho \approx 5\rho_0$. But since this term is essential for the chiral $SU(3)$ model to obtain reasonable values for the effective nucleon mass and the compressibility, this model predicts overcriticality only at very high densities.

Now we want to discuss the inclusion of baryonic spin-$\frac{3}{2}$ resonances and how these effect the behavior of dense hadronic matter. For the following investigations we consider the two parameter sets C_1 and C_2, which satisfactorily describe finite nuclei (Sec. 8). As stated before, the main difference between the two parameter sets is the coupling of the strange condensate to the nucleon and the Δ. While in C_2 this coupling is set to zero, in the case of C_1 the nucleon and the Δ couple to the ζ field. This leads to very different predictions for the behavior of dense nuclear matter. In the RMF models both coupling constants of the Δ-Baryon are freely adjustable. They can be constrained by the fact, that there that should be, e.g. no Δ's in the ground state of normal nuclear matter and a possible second minimum in the nuclear equation of state should lie above the saturation energy of normal nuclear matter. Furthermore QCD sum-rule calculations suggest, that the net attraction for Δ's in nuclear matter is larger than that of the nucleon. From these constraints one can extract a 'window' of possible parameter sets $g_{\Delta\sigma}, g_{\Delta,\omega}$ [44]. If the masses of the resonances are generated dynamically by the scalar condensate, like in the chi-
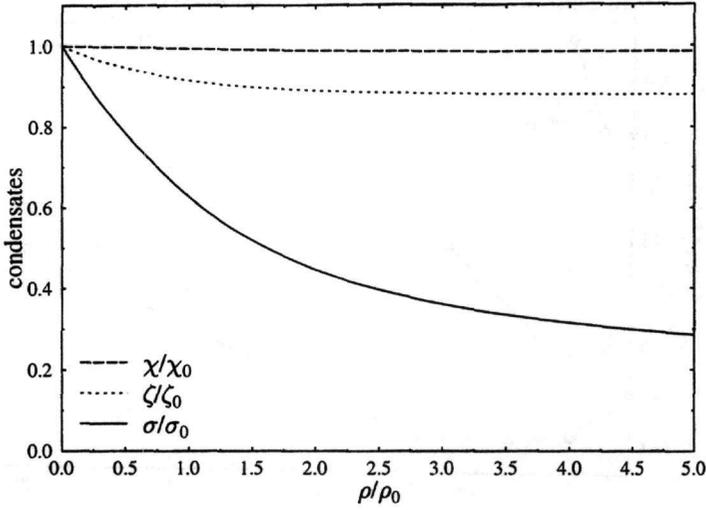
Fig. 12. Scalar condensates σ, ζ and χ as a function of the baryon density for zero net strangeness
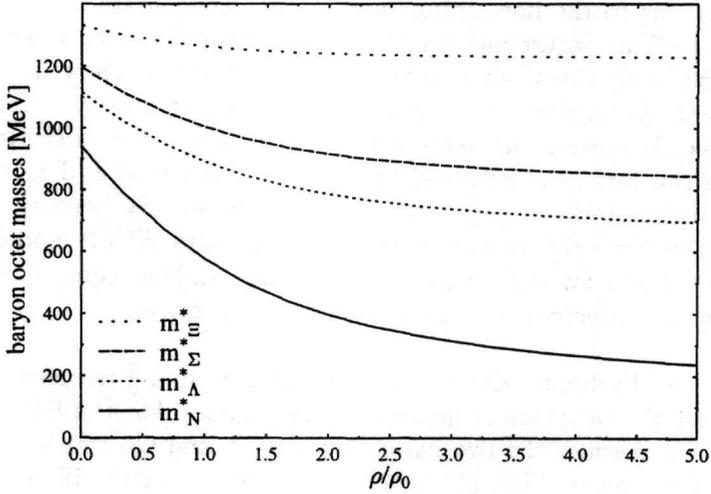

Fig. 13. Effective baryon masses as a function of the baryon density for zero net strangeness

ral model, then this coupling constant can be fixed. The vector coupling stays unfixed, but using the constraints from above one gets only a small region of possible values for $g_{\Delta\omega}$. In Fig. 19 we varied the $\Delta - \omega$ coupling to show the possible range for this value. In all other figures the ratio of the $N - \omega$ coupling to the $\Delta - \omega$ coupling is set to one. In Fig. 16 we show the equation of state for nuclear matter with and without the Δ-baryons for different parameter sets. One sees that around two times normal nuclear density the resonances influence the equation of state. But the strength of the influence depends on the strength of the coupling of the nucleon to the strange condensate ζ. This
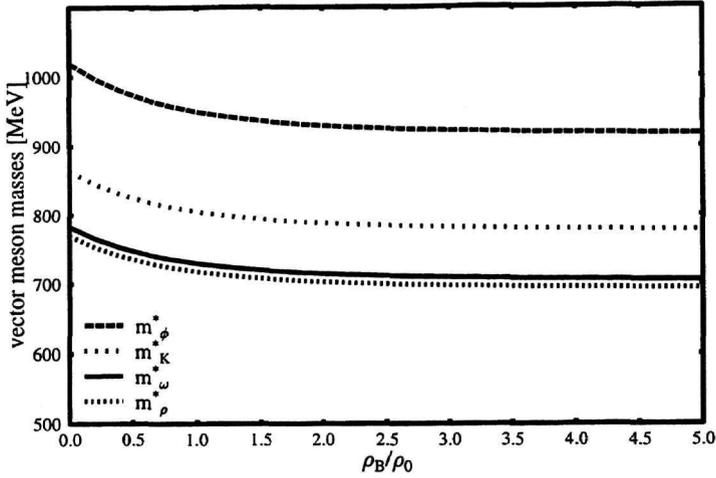
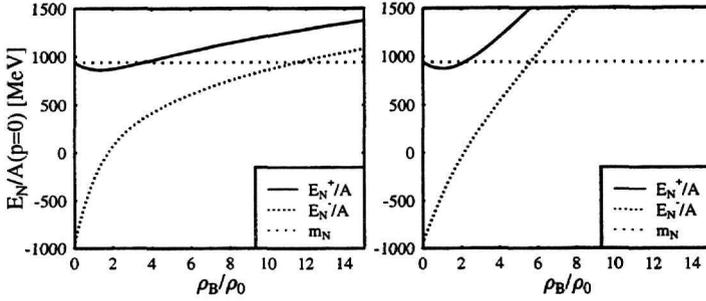Fig. 14. Vector meson masses as a function of density

Fig. 15. Nucleon and anti-nucleon energy at $\vec{p} = 0$ as a function of baryon density. On the left hand side parameter set C_1 was use, while on the right hand side the coupling constant g4 for the quartic vector meson interaction was set to zero

can be understood from Fig. 17 where the ratio of the effective Δ-mass to the effective nucleon-mass is displayed. If there is no coupling of the nucleon to the ζ field (C_2), the mass ratio stays constant but if the nucleon couples to the strange condensate (C_1) the situation changes. If one now looks at the ratio of the effective masses, Fig. 17, one sees that the ratio increases with density. That means the nucleon feels more scalar attraction than the Δ, which leads to reduced Δ production, as shown in Fig. 18. In Fig. 19 we vary the $\Delta - \omega$ coupling strength so that the ratio $r_v = g_{\Delta\omega}/g_{N\omega}$ is changed. One observes that a smaller value for this ratio leads to higher Δ-production, since they feel less repulsion, an this leads to an increasingly softened equation of state. The minimal value for r_v is fixed by the constraint, that the second possible minimum in the EOS should not be lower than normal nuclear matter ground state. This implies the minimal value $r_v = 0.68$ for C_1 and $r_v = 0.91$ for C_2. Here one needs further experimental or theoretical constraints to fix this coupling.
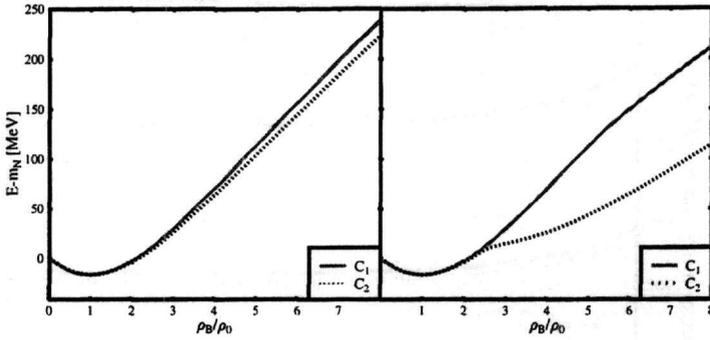
Fig. 16. Equation of state for infinite nuclear matter for the parameter sets C_1 and C_2. In the left picture resonances are neglected while they are included in the right picture. If the strange condensates couples to the nucleon the influence of the Δ resonances on the equation of state is much weaker
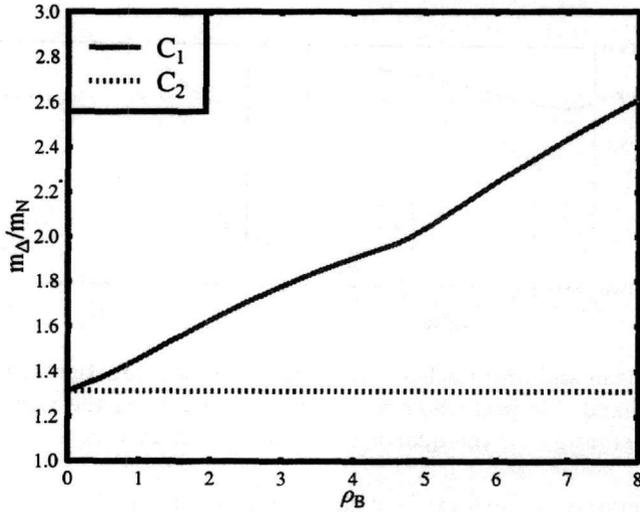

Fig. 17. Ratio of Δ-mass to nucleon-mass as a function of density for the two parameter sets C_1 and C_2

9.2 Extrapolation to finite temperatures

The extrapolation to finite temperatures is straight forward by using the grand canonical ensemble. Now the scalar densities ρ_i^s and the vector density ρ_i have the form

$$\rho_i^s = \gamma_i \int\limits_0^\infty \frac{d^3 k}{(2\pi)^3} \frac{m_i^*}{E_i^*} \left[\frac{1}{\exp\left(E_i^* - \mu_i^*\right)/T + 1} + \frac{1}{\exp\left(E_i^* + \mu_i^*\right)/T + 1} \right] ,$$
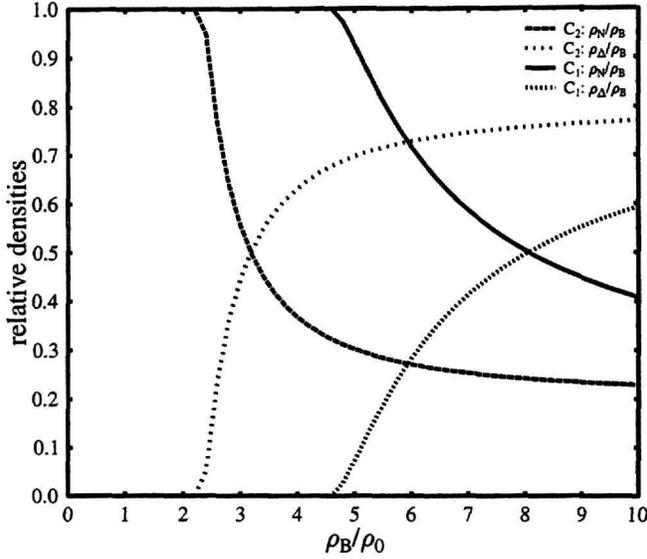
Fig. 18. Relative densities of nucleons and Δ's for various parameter sets. The production rate of Δ's depends strongly on the parameter set, i.e. on the strength of the nucleon-ζ and Δ-ζ coupling
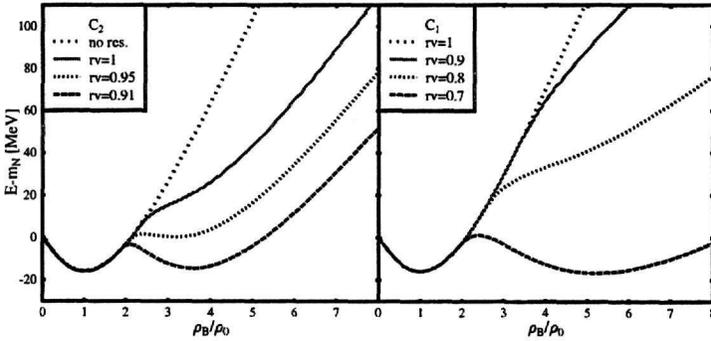

Fig. 19. Equation of state for parameter sets C_1 and C_2 for different values of the quotient $r_v = g_{N\omega}/g_{\Delta\omega}$. For the C_2-fit the value of r_v should not be less than 0.91 to avoid the density isomer being absolutely stable. For C_2, r_v must be larger than 0.68

$$\rho_i = \gamma_i \int\limits_0^\infty \frac{d^3k}{(2\pi)^3} \left[\frac{1}{\exp\left[(E_i^* - \mu_i^*)/T\right] + 1} - \frac{1}{\exp\left[(E_i^* + \mu_i^*)/T\right] + 1} \right] .$$

These have to be calculated numerically and inserted in the field equations (45) to determine the mesonic fields, the grand canonical potential and the thermodynamic quantities for given temperature and chemical potentials.

In Fig. 20 we show the behavior of the strange and non-strange condensates as functions of temperature for vanishing chemical potential with and without baryon resonances. One sees the important influence of the additional degrees
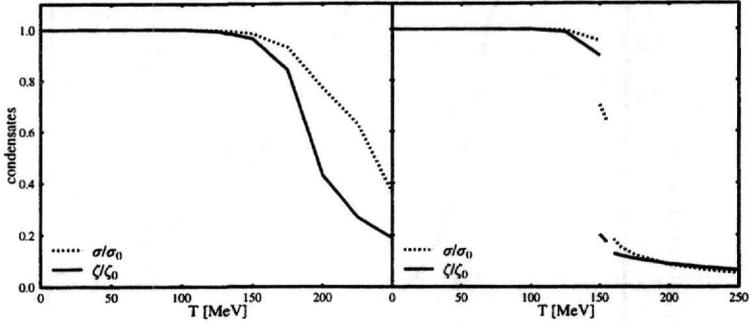
Fig. 20. Chiral condensates as a function of temperature for vanishing chemical potential. (**Left**) No resonances included. (**Right**) Baryon decuplet included
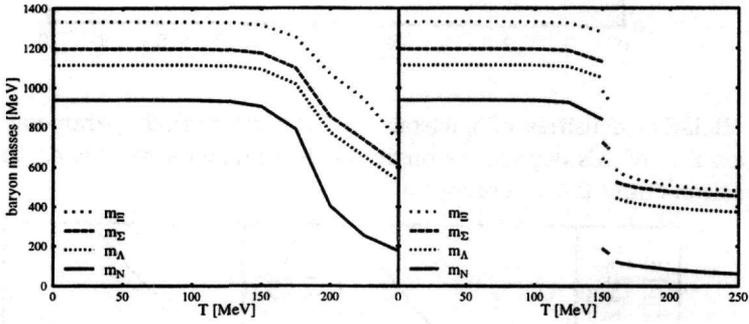

Fig. 21. Baryon octet masses as a function of temperature for vanishing chemical potential. (**Left**) No resonances included. (**Right**) Including baryon decuplet
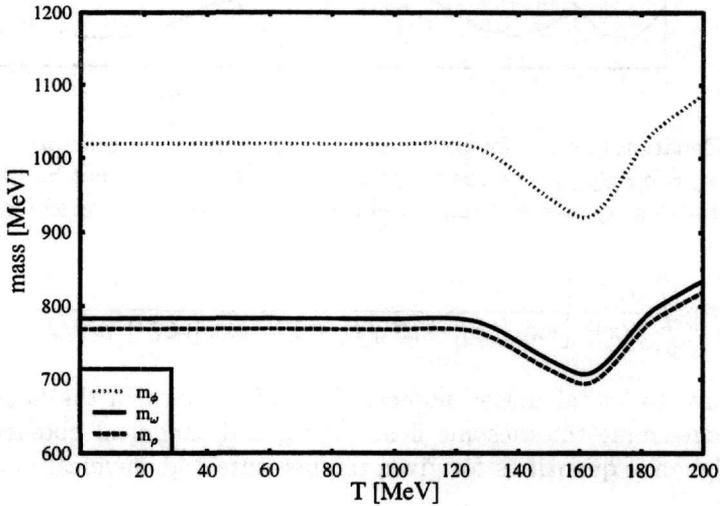

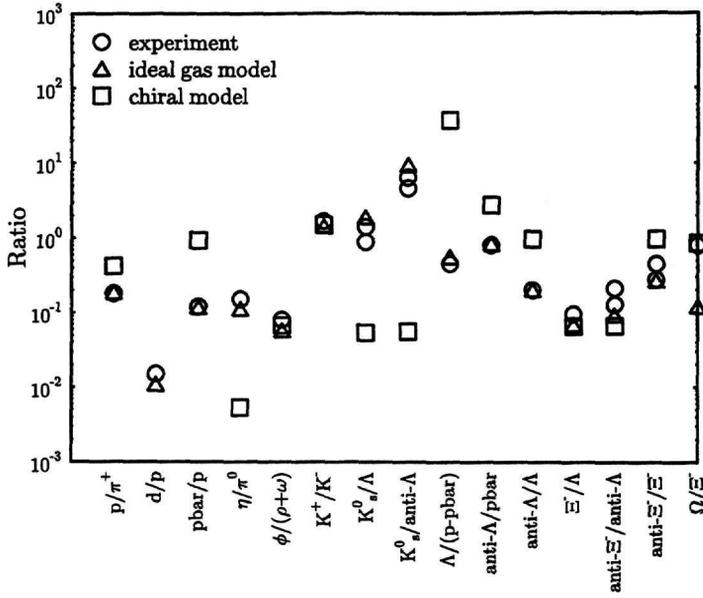Fig. 22. Vector meson masses as a function of temperature for vanishing chemical potential

Fig. 23. Particle ratios for 200 A GeV/c S+Au collisions using T=160 MeV and $\mu_q = 57$ MeV, $\mu_s = 24$ MeV

of freedom, since through the inclusion of the resonances the way how the chiral condensates change at high T are different. In the case that no resonances are included, one observes a smooth transition to small expectation values of the condensates, while for the case of included resonances both scalar fields jump to lower values. This is due to the much larger amount of degrees of freedom which accelerate the process of dropping condensates and increasing scalar density, which leads to further dropping condensates and again increasing scalar density. This scenario finally leads to a first order phase transition (actually there are two transitions, one for each scalar field, but they are in such a small region, that we will speak only of one transition). The resulting hadron masses as a function of temperature are shown in Figs. 21 and 22. As a final application we use the obtained temperature and chemical potentials for $S + Au$ collisions at an energy of 200 AGeV as obtained from a thermal model [45] an insert these to obtain the resulting particle ratios. The results in the chiral model, compared to the thermal model and the experimental yields are shown in Fig. 23. The resulting deviations are enormous. The change of the masses in the hot and dense medium (especially the baryon masses) leads to drastically altered particle ratios, and this raises the question whether at temperatures of more than 150 MeV the thermal model assumptions may be valid.

10 Conclusions

We reviewed the construction and application of an effective chiral $SU(3)$ model, which is based on QCD symmetries, namely chiral symmetry and scale invariance. The masses of the hadrons are generated by chiral condensates through the principle of spontaneous symmetry breaking. Only the pseudoscalar mesons (Goldstone bosons) acquire their mass by explicit symmetry breaking. Most of the meson-meson and baryon-meson coupling constants are constrained by some hadrons masses and basic nuclear matter saturation properties. As has be shown, this leads to a model, that offers the possibility to reproduce the full range of hadron masses and predict the properties of finite nuclei and excited nuclear matter. Since the model incorporates the $SU(3)$ hadronic multiplets the extrapolation the calculations into the strange sector is straight forward for all cases. The quantitative results for finite nuclei are being improved by a direct fit to finite nuclei. Further studies are under way to investigate the influence of the predicted behavior of hot and dense nuclear matter on observables in relativistic heavy ion collisions.

Acknowledgments

A Appendix

The $SU(3)$ matrices of the hadrons are (suppressing the Lorentz indices)

$$X = \frac{1}{\sqrt{2}}\sigma^a \lambda_a = \begin{pmatrix} (a_0^0 + \sigma)/\sqrt{2} & a_0^+ & \kappa^+ \\ a_0^- & (-a_0^0 + \sigma)\sqrt{2} & \kappa^0 \\ \kappa^- & \overline{\kappa^0} & \zeta \end{pmatrix}, \tag{A.1}$$

$$P = \frac{1}{\sqrt{2}}\pi_a \lambda^a \nu_1 \tag{A.2}$$

$$
= \begin{pmatrix}
\frac{1}{\sqrt{2}}\left(\pi^0 + \frac{\eta^8}{\sqrt{1+2\,w^2}}\right) & \pi^+ & 2\frac{K^+}{w+1} \\
\pi^- & \frac{1}{\sqrt{2}}\left(-\pi^0 + \frac{\eta^8}{\sqrt{1+2\,w^2}}\right) & 2\frac{K^0}{w+1} \\
2\frac{K^-}{w+1} & 2\frac{\overline{K}^0}{w+1} & -\frac{\eta^8\sqrt{2}}{\sqrt{1+2\,w^2}}
\end{pmatrix}, \tag{A.3}
$$

$$
V = \frac{1}{\sqrt{2}}v^a\lambda_a = \begin{pmatrix}
(\rho_0^0 + \omega)/\sqrt{2} & \rho_0^+ & K^{*+} \\
\rho_0^- & (-\rho_0^0 + \omega)/\sqrt{2} & K^{*0} \\
K^{*-} & \overline{K^{*0}} & \phi
\end{pmatrix}, \tag{A.4}
$$

$$
B = \frac{1}{\sqrt{2}}b^a\lambda_a = \begin{pmatrix}
\frac{\Sigma^0}{\sqrt{2}} + \frac{\Lambda^0}{\sqrt{6}} & \Sigma^+ & p \\
\Sigma^- & -\frac{\Sigma^0}{\sqrt{2}} + \frac{\Lambda^0}{\sqrt{6}} & n \\
\Xi^- & \Xi^0 & -2\frac{\Lambda^0}{\sqrt{6}}
\end{pmatrix}, \tag{A.5}
$$

for the scalar (X), pseudoscalar(P), vector (V), baryon (B) and similarly for the axial vector meson fields. A pseudoscalar chiral singlet $Y = \sqrt{2/3}\eta_0\mathbf{1}$ can be added separately, since only an octet is allowed to enter the exponential (14).

The notation follows the convention of the Particle Data Group (PDG) [46], though we are aware of the difficulties to directly identify the scalar mesons with the physical particles [47]. However, note that there is increasing evidence that supports the existence of a low-mass, broad scalar resonance, the $\sigma(560)$-meson, as well as a light strange scalar meson, the $\kappa(900)$ (see [48] and references therein).

The masses of the various hadrons are generated through their couplings to the scalar condensates, which are produced via spontaneous symmetry breaking in the sector of the scalar fields. Of the 9 scalar mesons in the matrix X only the vacuum expectation values of the components proportional to λ_0 and to the hypercharge $Y \sim \lambda_8$ are non-vanishing, and the vacuum expectation value $\langle X \rangle$ reduces to:

$$
\langle X \rangle = \frac{1}{\sqrt{2}}(\sigma^0\lambda_0 + \sigma^8\lambda_8) \equiv \mathrm{diag}\left(\frac{\sigma}{\sqrt{2}}, \frac{\sigma}{\sqrt{2}}, \zeta\right), \tag{A.6}
$$

in order to preserve parity invariance and assuming, for simplicity, $SU(2)$ symmetry [4] of the vacuum.

---

[4] This implies that isospin breaking effects will not occur, i.e., all hadrons of the same isospin multiplet will have identical masses. The electromagnetic mass break-

References

[1] J.D. Walecka, *Theoretical Nuclear and Subnuclear Physics*, Oxford University Press, New York (1995).

[2] B.D. Serot and J.D. Walecka, Adv. Nucl. Phys. **79**, 3612 (1997).

[3] J. Boguta and A.R. Bodmer, Nucl. Phys. **A292**, 413 (1977).

[4] R.J. Furnstahl, C.E. Price, and G.E. Walker, Phys. Rev. **C36**, 2590 (1987).

[5] E.K. Heide, S. Rudaz, and P.J. Ellis, Nucl. Phys. **A571**, 713 (1994).

[6] G. Carter, P.J. Ellis, and S. Rudaz, Nucl. Phys. **A603**, 367 (1996).

[7] R.J. Furnstahl, H.B. Tang, and B.D. Serot, Phys. Rev. **C52**, 1368 (1995).

[8] I. Mishustin, J. Bondorf, and M. Rho, Nucl. Phys. **A555**, 215 (1993).

[9] P. Papazoglou *et al.*, Phys. Rev. **C55**, 1499 (1997).

[10] J. Schechter, Phys. Rev. **D21**, 3393 (1980).

[11] N.A. Törnqvist, The linear $U(3) \times U(3)$ σ model, the $\sigma(500)$ and the spontaneous breaking of symmetries, e-print **hep-ph/9711483**.

[12] T. Waas and W. Weise, Nucl. Phys. **A625**, 287 (1997).

[13] V. Koch, Phys. Lett. **B337**, 7 (1994).

[14] P. Papazoglou *et al.*, Phys. Rev. **C57**, 2576 (1998).

[15] P. Papazoglou *et al.*, Nuclei in a chiral $SU(3)$ model, e-print **nucl-th/9806087**.

[16] R.E. Marshak, N. Mukunda, and S. Okubo, Phys. Rep. **B 699**, 137 (1965).

[17] M. Gell-Mann, Physics **1**, 63 (1962).

[18] B.L. Ioffe, Nucl. Phys. **B188**, 317 (1981).

[19] G.A. Christos, Phys. Rev. **D35**, 330 (1987).

[20] C.G. Callan, S. Coleman, J. Wess, and B. Zumino, Phys. Rev. **177**, 2247 (1969).

[21] S. Weinberg, *The Quantum Theory of Fields*, Volume 2, Cambridge University Press, Cambridge (1996).

[22] V.J.G. Stoks and T.A. Rijken, Nucl. Phys. A **613**, 311 (1997).

[23] J. Schechter, Y. Ueda, and G. Venturi, Phys. Rev. **177**, 2311 (1969).

[24] J.J. Sakurai, *Currents and Mesons*, University of Chicago Press, Chicago (1969).

[25] S. Gasiorowicz and D. Geffen, Rev. Mod. Phys. **41**, 531 (1969).

---

ing is neglected.

[26] P.K. Mitter and L.J. Swank, Nucl. Phys. **B8**, 205 (1968).

[27] P. Ko and S. Rudaz, Phys. Rev. **D50**, 6877 (1994).

[28] W.A. Bardeen and B.W. Lee, Phys. Rev. **177**, 2389 (1969).

[29] R.J. Furnstahl, B.D. Serot, and H.B. Tang, Nucl. Phys. **A598**, 539 (1996).

[30] J. Schechter and Y. Ueda, Phys. Rev. **D3**, 168 (1971).

[31] B.D. Serot and J.D. Walecka, Int. J. Mod. Phys. **E6**, 515 (1997).

[32] N. M. Hugenholtz and L. van Hove, Physica **24**, 363 (1958).

[33] R.J. Furnstahl and B.D. Serot, Phys. Rev. **C47**, 2338 (1993).

[34] P. Reinhard, Rep. Prog. Phys. **52**, 439 (1989).

[35] M. Rufa, Ph.D. thesis, J. W. Goethe–Universität, Frankfurt am Main (1989).

[36] C.E. Price, J.R. Shepard, and J.A. McNeil, Phys. Rev. **C41**, 1234 (1990).

[37] H. de Vries, C.W. de Jager, and C. de Vries, At. Data and Nucl. Data Tables **36**, 495 (1987).

[38] C. Beckmann *et al.*, in preparation (1999).

[39] R. J. Furnstahl, J.J. Rusnak, and B.D. Serot, Nucl. Phys. **A632**, 607 (1998).

[40] K. Rutz, Ph.D. thesis, J.W. Goethe Universität Frankfurt am Main, (1998).

[41] W. Brückner *et al.*, Phys. Lett. **B79**, 157 (1978).

[42] R. Bertini *et al.*, Phys. Lett. **B83**, 306 (1979).

[43] D.J. Millener, C.B. Dover, and A. Gal, Phys. Rev. **C38**, 2700 (1988).

[44] D. Kosov, C. Fuchs, and B. Martemyanov A. Faessler, PL **B421**, 37 (1998).

[45] P. Braun-Munzinger, J. Stachel, J.P. Wessels, and N. Xu, Phys. Lett. **B365**, 1 (1996).

[46] Particle Data Group (PDG), R. M. Barnett *et al.*, Phys. Rev. **D54**, 1 (1996).

[47] M. Harada and J. Schechter, Phys. Rev. **D54**, 3394 (1996).

[48] D. Black, A.H. Fariborz, F. Sannino, and J. Schechter, Evidence for a scalar $\kappa(900)$ resonance in πK scattering, e-print **hep-ph/9804273**.